https://doi.org/10.5194/egusphere-2024-556
Preprint. Discussion started: 18 March 2024

Improve *i*LOVECLIM (version 1.1) with a multi-layer snow model: surface mass balance evolution during the Last Interglacial

Thi-Khanh-Dieu Hoang[1], Aurélien Quiquet[1], Christophe Dumas[1], Andreas Born[2], and Didier M. Roche[1,3]

[1]Laboratoire des Sciences du Climat et de l'Environnement, LSCE/IPSL, CEA-CNRS-UVSQ, Université Paris-Saclay, 91191 Gif-sur-Yvette, France
[2]Department of Earth Sciences, University of Bergen and Bjerknes Centre for Climate Research, Bergen, Norway
[3]Department of Earth Sciences, Faculty of Science, Vrije Universiteit Amsterdam, Amsterdam, the Netherlands

Correspondence: Thi-Khanh-Dieu Hoang (dieu.hoang@lsce.ipsl.fr)

Abstract. During the Quaternary, ice sheets experienced several retreat-advanced cycles, strongly influencing climate patterns. In order to properly simulate these phenomena, it is preferable to use physics-based models instead of parameterizations to estimate surface mass balance (SMB) which has a strong influence on the ice sheet evolution. To further investigate the potential of these SMB models, this work evaluates BESSI (BErgen Snow Simulator), a multi-layer snow model with high computational efficiency, as an alternative to providing SMB for paleo studies. First, we validate the snow model using the regional climate model MAR (Modèle Atmosphérique Régional) as forcing and reference for the present-day climate over Greenland and Antarctic Ice Sheets. The evolution of SMB over the Last Interglacial period (LIG) (130-116 kaBP) is computed by forcing BESSI with transient climate forcing obtained from an Earth system model *i*LOVECLIM for both ice sheets. For present-day climate conditions, BESSI exhibits good performance compared to MAR despite a much simpler model set-up. The model also captures well the variation of SMB and its components during the LIG. Compared to the current simple melt estimation scheme of *i*LOVECLIM (ITM), BESSI is able to capture different SMB patterns for two particular ice sheet climate conditions thanks to its higher physical constraints while ITM displays a strong sensitivity to its parameters and input fields (temperature). The findings suggest that BESSI can provide more reliable SMB estimations for the *i*LOVECLIM framework to improve the model simulations of the ice sheet evolution and interactions with climate.

1 Introduction

The Quaternary (since 2.6 MaBP) has experienced several glacial-interglacial cycles. These episodic events influenced the whole Earth system, with climate shifting periodically from cold to warm phases and repeated retreat-advance cycles of the ice sheets and glaciers. Ice sheets and their interactions with climate strongly influence phenomena such as sea level evolution (Dutton et al., 2015; Spratt and Lisiecki, 2016; Turney et al., 2020) or changes in the atmospheric circulation (Ullman et al., 2014; Liakka et al., 2016). Ice sheets gain mass through surface accumulation (snow and rain) and internal accumulation (refreezing). In contrast, they lose mass due to melting and sublimation/evaporation processes on the surface or through iceberg calving and sub-shelf melting. The difference between mass gains and losses at the surface is called surface mass

https://doi.org/10.5194/egusphere-2024-556
Preprint. Discussion started: 18 March 2024

balance (SMB), which plays a significant role in the build-up or disappearance of the ice sheets. Studies of ice sheet evolution through past events unravel the dynamics of glaciation and deglaciation, improving trajectories of ice sheets in the past as well as confidence in future projections.

Investigating ice sheets and climate feedback in such long-time scales requires a tool that can simulate the interactions between the main components of the Earth system with reasonable computational cost. In this context, Earth system models of intermediate complexity (EMICs) are of interest as they have much lower computational costs compared to state-of-the-art general circulation models (GCMs) whilst still being able to simulate most of the important processes thanks to their low resolution and simplifications (Claussen et al., 2002; Eby et al., 2013). However, these simplifications result in some drawbacks, particularly in reproducing the evolution of ice sheets. Because of their coarse resolution, EMICs fail to capture the narrow ablation zones in the ice sheets' margin, leading to improper runoff estimation (Ettema et al., 2009; Noël et al., 2019). To mitigate this problem, the output of the atmospheric part can be bi-linearly interpolated (Gregory et al., 2012) or downscaled (Quiquet et al., 2021) to provide finer resolution input to the ice sheet model in the EMICs framework.

Another problem is the missing physical snow models within the EMICs framework to simulate the energy and mass transfer between the surface and the atmosphere (Lenaerts et al., 2019). In general, EMICs mostly utilize simple parameterizations such as positive degree day (PDD) (Reeh, 1991) or insolation temperature melt equation (ITM) (Van Den Berg et al., 2008) due to their simplicity and low computational cost (Born and Nisancioglu, 2012; Stone et al., 2013; Robinson and Goelzer, 2014; Goelzer et al., 2016b; Quiquet et al., 2021). However, as these schemes depend on locally calibrated parameters, their reliability is questioned when climate conditions change or when available data for calibration is limited, particularly in paleo studies. Bauer and Ganopolski (2017) report a failure of PDD in providing proper SMB values for the last glacial cycle study, which resulted from the absence of albedo feedback simulation. This poses a need to include a more physical snow model in such long-term climate simulations. The first option is sophisticated surface energy balance models (SEBs) included in regional climate models (RCMs) which have abilities to simulate not only the physically key processes of SMB (melt, sublimation and snow drifting) but also snow properties such as densities and metamorphism (Fettweis et al., 2017; Noël et al., 2018; Agosta et al., 2019; van Dalum et al., 2022). However, due to their complexity and computational cost, they are not suitable for long-term transient simulations and large study areas. As a compromise between parameterizations and SEB models, intermediate complexity energy balance models are promising SMB schemes for EMICs to run long simulations of ice sheet studies. These models have the appropriate level of simplicity in their structure and high computational efficiency, such as Born et al. (2019).

To answer the question of whether a physics-based scheme can improve the representation of SMB for paleo timescale, this work aims to assess the possibility of replacing the simple SMB scheme in *i*LOVECLIM with a physical-based surface energy balance model BESSI (Bergen Snow SImulator) (Born et al., 2019). Thanks to its high computational efficiency, *i*LOVECLIM has been used to carry out many paleoclimate studies ranging from ice sheet-climate interactions during the last deglaciation (Roche et al., 2014a; Quiquet et al., 2021; Bouttes et al., 2023), Heinrich Events (Roche et al., 2014b), to ocean circulation (Lhardy et al., 2021a) and carbon cycle changes between glacial-interglacial states (Bouttes et al., 2018; Lhardy et al., 2021b). BESSI is a surface energy and mass balance model designed for Earth system models of intermediate complexity. The snow model has been used to study a surface mass balance of the Greenland ice sheet during different periods (Zolles and

https://doi.org/10.5194/egusphere-2024-556
Preprint. Discussion started: 18 March 2024

Born, 2021; Holube et al., 2022; Zolles and Born, 2022) and proved to have good performance compared to other more complex models (Fettweis et al., 2020). In this work, we evaluate the performance of the updated version of BESSI since Zolles and Born (2021) for present-day climate using output from the regional climate model MAR (Modèle Atmosphérique Régional) as forcing and benchmark in Greenland and Antarctic Ice Sheets. By doing this, we assess the model's performance under different climate conditions and its ability to be applied to a new study area - Antarctica. In the second part, we assess the possibility of applying BESSI in a paleo simulation by using *i*LOVECLIM as a climate forcing. Next, we compare BESSI to ITM - the current SMB scheme of *i*LOVECLIM to investigate the differences between the two models. We select the most recent interglacial period (LIG) (130-116 kaBP), which corresponds to the marine isotope stage (MIS) 5e. During this period, as the summer insolation in the Northern Hemisphere increases due to the change in the orbit of the Earth, the annual global mean temperature is about 2 degrees Celsius higher in the annual global mean temperature than the pre-industrial period (Kukla et al., 2002; Turney and Jones, 2010; Otto-Bliesner et al., 2013), inducing retreats of ice sheets and glaciers (Dutton and Lambeck, 2012; Dyer et al., 2021). Hence, the LIG provides documented records and insights into the behaviors of different Earth system components under warm climates to benchmark models and study the dynamics behind the phenomena (Fischer et al., 2018). This period has been well-studied for various aims such as reconstructing temperature (Lunt et al., 2013; Landais et al., 2016; Obreht et al., 2022) and sea level (Kopp et al., 2013; Dutton et al., 2015); investigating climate and ice-sheet interactions (Bradley et al., 2013; Goelzer et al., 2016a; Sutter et al., 2016). Applying BESSI for the LIG has been done before in the work of Plach et al. (2018) for the Greenland Ice Sheet only by using climate forcings from MAR with equilibrium runs of some LIG time slices: 130, 125, 120, and 115 kaBP. In our work, as *i*LOVECLIM is much more computationally inexpensive compared to MAR, we can run the model transiently to investigate the evolution of SMB throughout the whole LIG period. For this work, we select the LIG to investigate the abilities of ITM and BESSI in reproducing the SMB under different boundary conditions (deglaciation and glacial inception). From this, we can fully evaluate the advantage of using a more physics-based model in simulating SMB for an intermediate complexity Earth model.

Section 2 provides background information about the models and the climate forcings, together with the design of the experiments. The results are presented in Sect. 3, followed by a discussion about the model's performance in Sect. 4. Finally, a summary of the work is in Sect. 5.

2 Methods

2.1 Models description

2.1.1 BESSI

Bergen Snow SImulator - BESSI is a multi-layer snow model simulating the surface energy and mass balance with high computational efficiency, designed to be coupled with low-resolution Earth system models (Born et al., 2019). The model, which in its current configuration uses 15 vertical snow layers, requires near-surface air temperature, total precipitation, humidity, surface pressure, and downward long-/short-wave radiation in daily timestep as input. From the forcings, the model simulates

https://doi.org/10.5194/egusphere-2024-556
Preprint. Discussion started: 18 March 2024

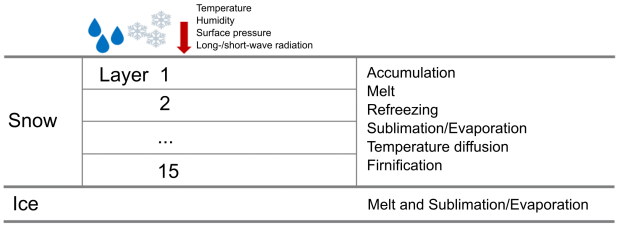

Figure 1. Sketch of BESSI model with required inputs and simulated processes

Table 1. Table of constant parameters of BESSI model

Parameter	Symbol	Value	Unit
Albedo of firn	α_{firn}	0.7	-
Albedo of fresh snow	$\alpha_{freshsnow}$	0.82	-
Albedo of ice	α_{ice}	0.4	-
Coefficient of sensible heat flux	D_{sh}	15	W m^{-2} K^{-1}
Emissivity of the surface	ϵ_s	0.98	-
Density of water	ρ_w	1000	kg m^{-3}
Heat capacity of air	c_a	1003 at 0°C	J kg^{-1} K^{-1}
Heat capacity of ice	c_i	2110 at -10°C	J kg^{-1} K^{-1}
Heat capacity of water	c_w	4181 at 25°C	J kg^{-1} K^{-1}
Latent heat of melting	L_m	3.34×10^5	J kg^{-1}
Latent heat of vaporization	L_v	2.5×10^6	J kg^{-1}
Ratio of latent and sensible heat	$r_{lh/sh}$	1.0	-
Stefan-Boltzmann constant	σ	5.670373×10^{-8}	W m^{-2} K^{-4}

90 important processes of surface mass balance, such as melt, refreezing, runoff, and sublimation/evaporation. Among the snow layers, heat diffusion and mass compaction are also simulated (Fig. 1). Full details on the implementation of these two processes are given in Born et al. (2019). In the following, we only detail the methodology used for surface energy and mass balance.

Surface energy balance

95 The exchange of energy between the surface (the top layer of the model) and the atmosphere resulted in the change of temperature in this layer (T_s), influenced by the net solar flux Q_{SW}, the net longwave radiation flux Q_{LW}, the sensible heat flux Q_{SH}, the latent heat flux Q_{LH}, the heat flux from the precipitation Q_{precip} and the melting flux Q_{melt} (when temperature reaches

https://doi.org/10.5194/egusphere-2024-556
Preprint. Discussion started: 18 March 2024

melting point). This can be expressed as follows

$$c_i m_{top} \left.\frac{\partial T_s}{\partial t}\right|_{surface} = Q_{SW} + Q_{LW} + Q_{SH} + Q_{LH} + Q_{precip} + Q_{melt} \quad (1)$$

in which, c_i is the heat capacity of ice (2110 J kg^{-1}K^{-1} at -10°C) and m_{top} is the mass of the top layer in kg m^{-2}.

The net incoming solar radiation Q_{SW} is calculated from the albedo of the surface (α_{snow} or α_{ice}) and the incoming shortwave radiation F_{SW} (Wm^{-2}) available from the forcing:

$$Q_{SW} = (1-\alpha)F_{SW} \quad (2)$$

The albedo of ice α_{ice} is fixed at 0.4 while the albedo of snow α_{snow} is calculated considering the exponential decay with time since the last snowfall event (Oerlemans and Knap, 1998; Zolles and Born, 2021):

$$\alpha_{snow} = \alpha_{firn} + (\alpha_{freshsnow} - \alpha_{firn}) exp\left(\frac{-N_{snowfall}}{t*}\right) \quad (3)$$

in which the albedo of firn α_{firn} is 0.7, the albedo of the fresh snow $\alpha_{freshsnow}$ is 0.82, $N_{snowfall}$ is the number of days since the last snowfall event and $t*$ is the number of days for the fresh snow to reach firn condition. Depending on the temperature T_{air}, $t*$ is set to 20 days for T_{air} < 273.15 K or 5 days for T_{air} = 273.15 K.

The difference between the upcoming longwave radiation F_{LW} from the atmosphere (read from the input) and the emitted longwave radiation flux is the net longwave radiation Q_{LW}:

$$Q_{LW} = F_{LW} - \sigma \epsilon_s T_s^4 \quad (4)$$

in which, σ is the Stefan-Boltzmann constant (5.670373 × 10^{-8} W m^{-2} K^{-4}), ϵ_s is the emissivity of the surface (0.98).

The turbulent sensible heat flux Q_{SH} equals to the difference between the temperature of the air T_{air} and that of the surface T_s multiplied by a coefficient D_{sh} (15 W m^{-2} K^{-1}):

$$Q_{SH} = D_{sh}(T_{air} - T_s) \quad (5)$$

The turbulent latent heat flux Q_{LH} depends on the difference between the water vapor pressure of the air e_{air} and of the surface e_s (calculated from the humidity), the surface pressure p_{air} from input and a coefficient D_{lh}:

$$Q_{LH} = \frac{D_{lh}}{p_{air}}(e_{air} - e_s) \quad (6)$$

$$\text{with } D_{lh} = 0.622 r_{lh/sh} \frac{D_{sh}}{c_a}(L_v + L_m) \quad (7)$$

where $r_{lh/sh}$ is the ratio of the exchange rates between the latent heat and sensible heat (equal to 1.0 in this work), c_a is the heat capacity of the air (1003 J kg^{-1} K^{-1} at 0°C) whilst L_v and L_m are latent heat of vaporization and melting, respectively (2.5×10^6 J kg^{-1} and 3.34×10^5 J kg^{-1}). Details of the turbulent sensible and latent heat fluxes calculation methods are available in Zolles and Born (2021).

https://doi.org/10.5194/egusphere-2024-556
Preprint. Discussion started: 18 March 2024

Based on the air temperature (T_{air}), BESSI classifies total precipitation as snow ($T_{air} \leq 273.15$ K) or rain ($T_{air} > 273.15$ K). When snow/rain falls, the air temperature is transported to the surface. Hence, the heat flux from the precipitation is different for snow and rain:

$$Q_{precip,s} = Precip \times \rho_w c_i (T_{air} - T_s) \quad (8)$$

$$Q_{precip,r} = Precip \times \rho_w c_w (T_{air} - 273.15) \quad (9)$$

where ρ_w is the density of water (1000 kg m^{-3}) and c_w is heat capacity of water (4181 J kg^{-1} K^{-1} at 25°C).

The model uses an implicit scheme, for which the energy fluxes are calculated first, then the energy required to heat the top layer to the melting point. As the temperature of the surface cannot exceed the melting point, the remaining energy is considered as energy available to melt snow/ice Q_{melt} (Eq. (1)). The main parameters of the model are presented in Table 1.

Surface mass balance

Surface mass balance SMB is an important element of the ice sheet mass balance, apart from the ice discharge and basal melting. In BESSI, SMB is calculated as the remaining mass of total precipitation from runoff and sublimation/evaporation processes:

$$SMB = Precip - (m_{runoff} + m_{sub}) \quad (10)$$

In BESSI, the incoming precipitation (rain/snow) accumulates first on the surface (Fig. 1). Generally, the precipitation adds snow mass to the top snow layer ($T_{air} \leq$273.15 K) or liquid mass to the water content of the surface (T_{air} > 273.15 K). As more snow accumulates in the top layer, BESSI generates new snow layers below to prevent the mass of the layer from exceeding the maximum threshold (500 kg m^{-2}). The mass of the new layer is set at 300 kg m^{-2}, and the old layer keeps the remaining mass, continuing to accumulate snow. Depending on the precipitation and the temperature, up to 15 layers can be formed. When more than one layer exists, the masses of these layers are shifted down to leave space for the new forming layer. In contrast, when Q_{melt} is available, the snow column melts from the top. To prevent the mass of the surface layer from sinking below the minimum threshold (100 kg m^{-2}), BESSI merges this layer with the next one. After the merging, the masses of the layers below are shifted up.

The water resulting from melt and rain is retained by the snow column up to 10% of its pore volume. The excess water percolates through the snow column, either refreezing due to low temperatures or leaving the lowest layer as runoff. The energy for refreezing, according to the assumption that the snow and the liquid water inside the snowpack are in thermodynamic equilibrium (Born et al., 2019), is calculated as:

$$Q_{refreezing} = c_i m_s (273.15 - T_{snow}) \quad (11)$$

in which T_{snow} is the temperature of the snow layer where the process takes place. Refreezing can occur anywhere among the snow layers, unlike melt, which happens only at the top.

https://doi.org/10.5194/egusphere-2024-556
Preprint. Discussion started: 18 March 2024

In case Q_{melt} is enough to melt all the snow layers, ice starts to melt, adding water to the runoff. Hence, the mass of runoff, which is the resulting amount of water from processes of rain, melt, and refreezing, is calculated as below:

$$\frac{\partial m_{runoff}}{\partial t} = Precip \times \rho_w + \frac{Q_{melt} - Q_{refreezing}}{L_m} \tag{12}$$

Sublimation/Evaporation, depending on the humidity of the air, is converted from the turbulent latent heat flux Q_{LH} to mass as:

$$\frac{\partial m_{sub}}{\partial t} = -\frac{Q_{LH}}{L_v + L_m} \tag{13}$$

Positive values indicate sublimation/evaporation happens, subtracting mass from SMB. On the contrary, deposition/condensation occurs, adding mass to SMB. Additional details on these calculations are available in Born et al. (2019) and Zolles and Born (2021).

2.1.2 *i*LOVECLIM

The Earth system model of intermediate complexity *i*LOVECLIM (version 1.1) is a code fork of the LOVECLIM 1.2 model originated from Goosse et al. (2010). The key components of the model include the modules ECBILT for the atmosphere, CLIO for the ocean, and VECODE for the vegetation. ECBILT is a quasi-geostrophic atmospheric model that runs on a T21 spectral grid (Opsteegh et al., 1998). Meanwhile, CLIO is a 3D free-surface ocean general circulation model coupled to a thermodynamic sea-ice model and discretized on $3^\circ \times 3^\circ$ spherical grid (Goosse and Fichefet, 1999). VECODE is a dynamical vegetation model that allocates carbon and simulates land cover and tree fraction on the same grid as the atmospheric model (Brovkin et al., 1997). *i*LOVECLIM runs with a 360-day calendar.

In terms of the SMB scheme, *i*LOVECLIM used the insolation temperature melt method (ITM) (Van Den Berg et al., 2008). This module is developed to provide SMB to the ice sheet model embedded in *i*LOVECLIM named GRISLI (Roche et al., 2014a) for coupling purposes (Quiquet et al., 2021). This parameterization calculates the melt water $Melt$ as

$$\frac{\partial Melt}{\partial t} = \frac{1}{\rho_w L_m}((1-\alpha_s)SW + c + T_s\lambda) \tag{14}$$

in which, ρ_w is liquid water density (1000 kgm^{-3}), L_m is the specific latent heat of melting (3.34×10^5 J kg^{-1}), α_s is the surface albedo, SW is the surface shortwave radiation and T_s is the surface temperature. Here, we used λ = 10 W m^{-2} K^{-1}, similar to Quiquet et al. (2021). For the empirical parameter c, we use c = -25 W m^{-2}. Considering the temperature bias of *i*LOVECLIM, Quiquet et al. (2021) carried out local modification to the parameter c according to the annual mean temperature bias compared to ERA-Interim (Dee et al., 2011). Quiquet et al. (2021) also implemented an albedo interpolation to take into account the altitude of the grid points (vertical) and to create a smooth transition of albedo value from ocean to land area (horizontal). Here, to provide a comparable ITM to BESSI, these albedo modifications are not included.

The equation of SMB (Eq.10) in this case is calculated as:

$$SMB = Precip - Melt \tag{15}$$

https://doi.org/10.5194/egusphere-2024-556
Preprint. Discussion started: 18 March 2024

Climate forcings for BESSI are obtained from the online downscaling module within *i*LOVECLIM framework, which recomputes the surface energy budget and total precipitation on a subgrid resolution for the ice sheet areas (Quiquet et al., 2018). This downscaling module is only carried out for land grid boxes. In this work, we run the downscaling for two polar regions to obtain near-surface air temperature, total precipitation, and humidity on a 40km×40km Cartesian grid (referred to as NH40 and SH40 for the North and South Poles, respectively). To obtain other input variables for BESSI, long-/short-wave radiation, and surface pressure are bi-linearly interpolated from the native T21 grid to the NH40/SH40 grid.

2.2 Present-day climate reference data

For calibration/validation purposes, we use the present-day climate data from one of the state-of-the-art regional climate models - MAR (Modèle Atmosphérique Régional). MAR has been widely applied to study the SMB changes and surface melt for polar regions (Fettweis et al., 2017; Agosta et al., 2019; Mankoff et al., 2021). The model, with a typical sub-daily time step of 120 s Fettweis (2007)), includes a 3D atmospheric model coupled with a 1D surface-atmosphere energy mass exchange scheme named SISVAT (Soil Ice Snow Vegetation Atmosphere Transfer) (Fettweis et al., 2017) that is more complex and physical than BESSI. It can simulate up to 30 layers of snow/ice and consider snow properties and metamorphism (Kittel et al., 2021). Also, the simulated surface albedo takes into account more variables, including snow's optical properties, clouds, snow depth, the presence of bare ice, and liquid water (Tedesco et al., 2016). Detailed about the MAR model and its setup can be found in Fettweis (2007) and Fettweis et al. (2013).

In this study, MAR acts as present-day forcing and reference benchmarks to compare with BESSI for both Greenland and Antarctic Ice Sheets (denoted as GrIS and AIS, respectively). The resolution of the climate forcings is 15km×15km for GrIS (version 3.13) and 35km×35km grid for AIS (version 3.12), covering the period 1979 - 2021.

2.3 Study design

In this work, we carry out two sets of experiments corresponding to the two climate forcings: MAR and *i*LOVECLIM.

In the first experiment, we investigate the performance of BESSI for present-day climate by using MAR as forcing (BESSI-MAR). The SMB calculated by MAR itself is used as a reference. The calibration and validation are carried out for GrIS and AIS during the study period from 1979 to 2021. Initially, the snow model is spun up by looping the forcing several times until it reaches an equilibrium state with an ice sheet mask of present-day extent, classified in MAR as grid cells with more than 50% of permanent ice. Some of BESSI's parameters, including $\alpha_{freshsnow}$, α_{firn}, α_{ice}, $r_{lh/sh}$ and D_{sh} are tuned to obtain lowest RMSE between BESSI and MAR output and narrowest gap in term of total SMB (SMB integrated over the ice sheet mask). The final values of these parameters are presented in Table 1. The 43-year mean SMB value from GrIS and AIS run is then analyzed. For validation, we use several goodness-of-fit metrics, such as coefficient of determination R^2, Root Mean Squared Errors (RMSE), and Normalized Root Mean Squared Errors (NRMSE) to assess BESSI-MAR performance refer to MAR (see Appendix A).

In the second set of experiments, we force the snow model by downscaled *i*LOVECLIM (BESSI-*i*LOVECLIM) to evaluate the possibility of replacing the current SMB scheme - ITM with BESSI. We run BESSI-*i*LOVECLIM for three different

https://doi.org/10.5194/egusphere-2024-556
Preprint. Discussion started: 18 March 2024

periods: the pre-industrial, the present-day, and the Last Interglacial. For each period, BESSI is always first spun up by looping the forcings several times for the snowpack to reach equilibrium before results are obtained for analysis.

First, BESSI-*i*LOVECLIM is run for the pre-industrial to provide a reference for the calibration of ITM. As the ITM version used here is different from Quiquet et al. (2021), we obtain the value for the melt parameter c in Eq.15 by tuning it aiming at the minimum RMSE between the climatological annual mean SMB of ITM and BESSI and the lowest difference in annual mean total SMB of the two models for the pre-industrial period (PI). By doing this, the comparison between ITM and BESSI for the LIG is more robust as the performance of the two models is similar for the PI. To obtain climate forcing for BESSI, we run downscaled *i*LOVECLIM for 50 years from a 1000-year spin-up under pre-industrial boundary conditions.

Due to its coarse resolution and simplification in physics, *i*LOVECLIM displays some incorrect climate patterns. Particularly, Heinemann et al. (2014) reported bias in surface air temperature of *i*LOVECLIM compared to observation in North America and Northern Europe, which are preserved in the downscaling version NH40 (Quiquet et al., 2018). To understand the impacts of climate in *i*LOVECLIM on the performance of the snow model, the comparison between BESSI-*i*LOVECLIM and BESSI-MAR is carried out for the present-day period. *i*LOVECLIM forcings for present-day is obtained by running the model with the prescribed greenhouse gases (GHG) concentrations during the same period as MAR, 1979-2021.

Finally, to evaluate the feasibility of applying BESSI for paleoclimate studies, SMB evolution during the LIG is simulated by BESSI-*i*LOVECLIM. At first, we run *i*LOVECLIM transiently during the LIG, 135-115 kaBP, with present-day ice sheet topography and varying orbital configuration and concentrations of GHG to obtain restart files. Then, for every 500 years, we sample 50 years of climatological daily output to provide forcings for BESSI. In total, we have 41 time slices covering the entire LIG period. Next, for each time slice, we run BESSI for 100 years from the spin-up of 135 kaBP and take the annual mean of the last 50 years for further analysis. In order to assess the trend of SMB evolution, we compute the differences in the annual mean SMB during the LIG with respect to the PI value for both BESSI-*i*LOVECLIM and ITM. The evolution of SMB simulated by BESSI and ITM during the LIG is then compared to investigate the models' performance.

3 Results

3.1 BESSI validated by present-day forcings from MAR

The map of the annual mean SMB simulated by the BESSI and MAR for Greenland during the period 1979 - 2021 is presented in Fig. 2a. Generally, the 43-year mean SMB simulated by BESSI is in good agreement with MAR despite a simpler model structure. Particularly, in the center of the ice sheet, where sublimation/evaporation is dominant due to dry climate, the SMB is simulated correctly by BESSI as referred to MAR (Supplementary Fig. S1a). However, in the southwest of Greenland, the ablation zone extent is noticeably underestimated in BESSI, which is also reported by Plach et al. (2018); Fettweis et al. (2020). Even though the extent is underestimated, the magnitude of ablation in BESSI is higher than MAR around the margins, particularly in the North and West of Greenland. For Antarctica, the SMB simulated by the two models also shows high agreement (Fig. 2b). The problem related to melting in Greenland is limited in this ice sheet as it has a much colder climate

https://doi.org/10.5194/egusphere-2024-556
Preprint. Discussion started: 18 March 2024

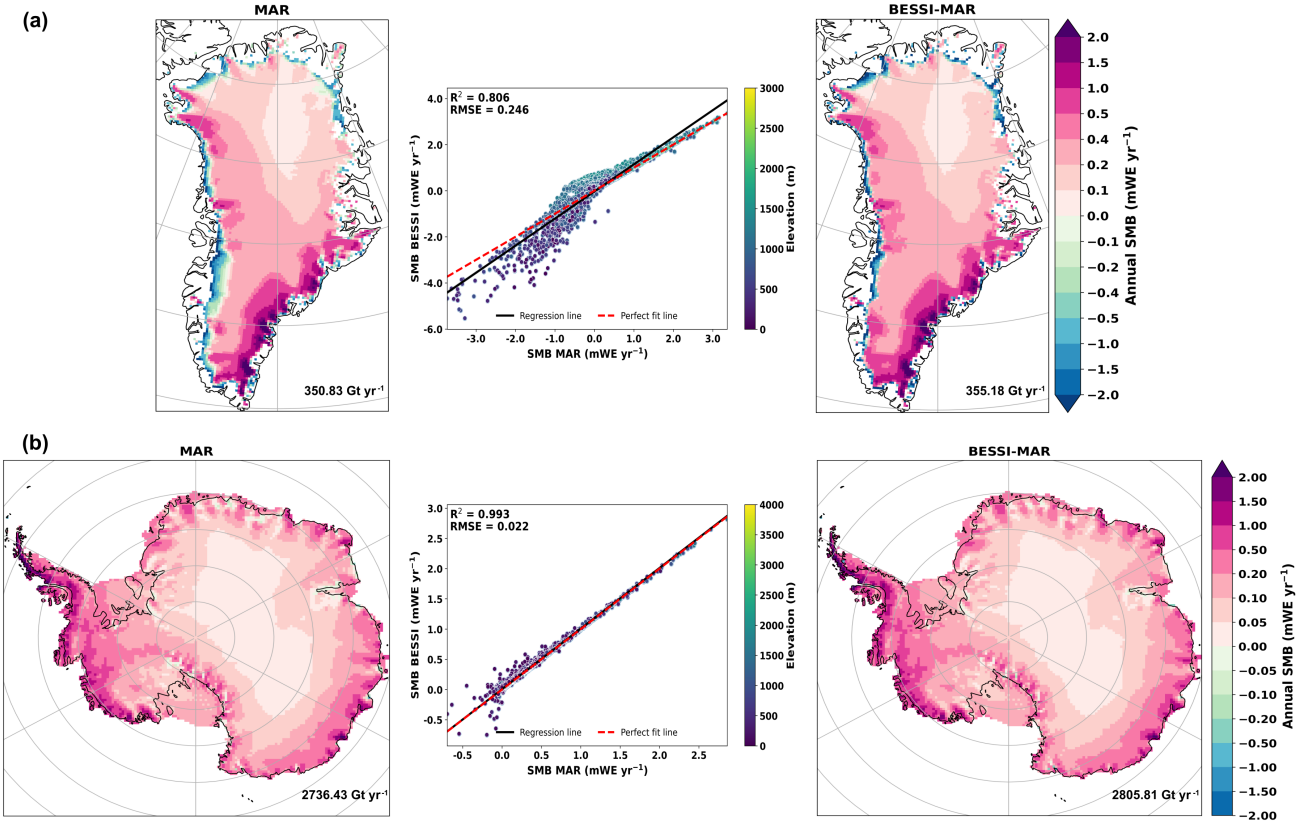

Figure 2. Annual mean SMB values (in mWE yr^{-1}) of MAR and BESSI in (row **a**) Greenland and (row **b**) Antarctica. The total SMB (in Gt yr^{-1}) integrated for the ice sheet area is also included. The grid points from the maps are plotted with elevation classification in the scatter plots, including the linear regression line in red and the perfect fit line (1,1) in dashed black.

(Supplementary Fig. S1b). In terms of total SMB, the difference between the two models is in an acceptable range: 1.24% for GrIS and 2.54% for AIS.

The scatter plots of the grid points with different elevations in the maps are also presented in Fig. 2, with the evaluation metrics to illustrate the goodness-of-fit between the two models for both ice sheets. For GrIS, BESSI tends to underestimate
255 SMB of the low-elevation grid points located in the ice sheet margin in the North and West (Fig. 2a). On the other hand, for points located near the equilibrium line (with SMB ≈ 0), SMB is slightly overestimated. Unlike GrIS, the scatter plot of AIS shows no under-/over-estimation in the mean SMB, consistent with the SMB map (Fig. 2b). In general, the evaluation metrics illustrate a good fit between BESSI and MAR for both ice sheets, with AIS slightly better. In particular, the coefficient of determination R^2 in AIS is 0.993 while that in GrIS is 0.806; RMSE is 0.022 for AIS and 0.246 for GrIS (unit here is mWE
260 yr^{-1}).

https://doi.org/10.5194/egusphere-2024-556
Preprint. Discussion started: 18 March 2024

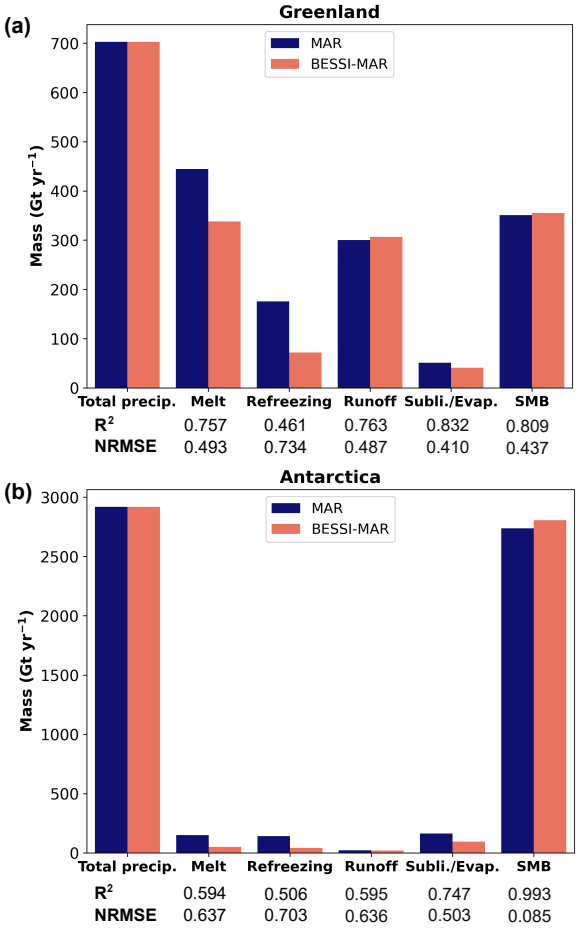

Figure 3. Contribution of different key processes to the 43-year mean total SMB in (**a**) Greenland and (**b**) Antarctica (in Gt yr^{-1}), with corresponding R^2 and NRMSE.

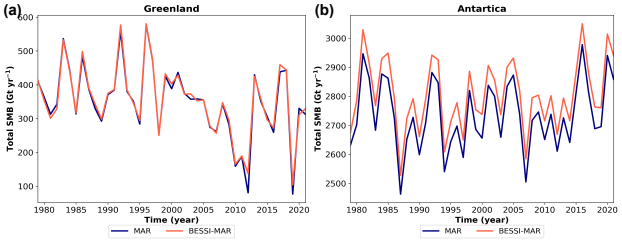

Figure 4. Temporal variation of the yearly mean total SMB integrated on present-day ice sheet extent (in Gt yr^{-1}) during 1979-2021 for (**a**) Greenland and (**b**) Antarctica.

https://doi.org/10.5194/egusphere-2024-556
Preprint. Discussion started: 18 March 2024

BESSI's performance in simulating key processes of SMB in Greenland is presented in Fig.3a. This bar chart illustrates the mean value of total SMB elements with the corresponding evaluation metrics: R^2 and NRMSE. We can see strong underestimations in melt and refreezing in BESSI, especially refreezing with less than half of MAR's value. This might result from the model's daily timestep, which causes the model to neglect the diurnal temperature cycle (Krebs-Kanzow et al., 2018). These underestimations are compensated in the runoff, leading to an acceptable value in BESSI compared to MAR. Among these major processes of SMB, refreezing, with the lowest R^2 (0.461) and highest NRSME (0.734), is not simulated as well as other processes. Sublimation/Evaporation, on the other hand, is shown to be well simulated with R^2 (0.832) and NRSME (0.41). The results of BESSI in Antarctica are not much different (Fig. 3b). As discussed above, the contribution of runoff to total SMB in this ice sheet is very small due to cold climate conditions. On the other hand, sublimation/evaporation differences between BESSI and MAR are larger than in Greenland as they are more dominant in Antarctica. This leads to slightly higher differences between the total SMB of the two models.

The variation of total SMB of the two ice sheets throughout the studied period is shown in Fig. 4. The figure shows that the temporal variation of total SMB is well captured in BESSI. For both cases, there is an overestimation of the total SMB in BESSI in comparison to MAR. In Greenland, BESSI reproduces the total SMB in very good accordance with that of MAR (Fig. 4a). Meanwhile, for Antarctica, the gap is slightly larger (Fig. 4b), which is consistent with the gap in the annual mean total SMB shown in Fig. 2b and Fig. 3b. However, considering the magnitude of total SMB in AIS, this small difference is deemed acceptable.

3.2 BESSI with *i*LOVECLIM as climate forcing

3.2.1 Climate in *i*LOVECLIM

Greenland

*i*LOVECLIM has a coarser resolution and simpler model setup than MAR - a state-of-the-art regional climate model used to calibrate/validate BESSI. This difference in the simulated climate strongly influences the performance of the snow model. The comparison of the climate of MAR and *i*LOVECLIM in terms of precipitation, temperature, and relative humidity is shown in Fig. 5. In general, the native T21 grid pattern is clearly visible in *i*LOVECLIM climate as the downscaling mostly redistributes climatic variables of the coarse resolution according to the subgrid topography (Quiquet et al., 2018). Also, it is noticeable that some ice sheet areas are not covered due to the coarse land grid boxes of the native T21 grid. Compared to MAR, *i*LOVECLIM has a higher annual mean precipitation rate in the South and in the center North of GrIS (Fig. 5a). Hence, the total precipitation is larger in *i*LOVECLIM with a gap of more than 200 Gt yr^{-1} (Table 2). In addition, the climate simulated by *i*LOVECLIM is generally warmer and less humid than MAR as *i*LOVECLIM has a higher range of annual mean near-surface temperature and a significantly lower humidity value (Fig. 5b and 5c). However, considering a much coarser original resolution of *i*LOVECLIM, it can still properly produce the climate major pattern in the right order of magnitude, except for humidity in Greenland after downscaled to a 40km×40km grid.

https://doi.org/10.5194/egusphere-2024-556
Preprint. Discussion started: 18 March 2024

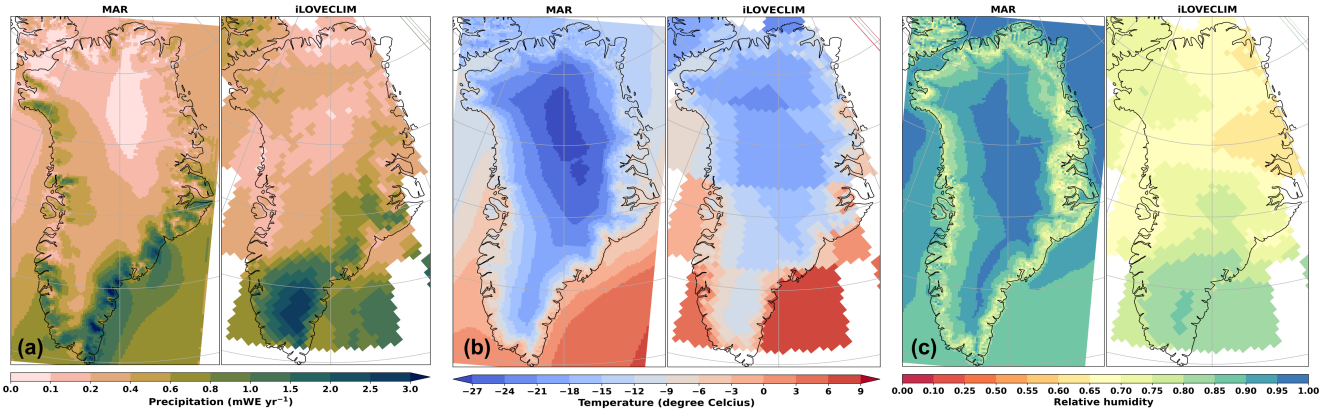

Figure 5. Annual mean value of climate variables including (**a**) precipitation (in mWE yr^{-1}), (**b**) near-surface temperature (in degree Celsius) and (**c**) relative humidity of MAR and *i*LOVECLIM for Greenland Ice Sheet.

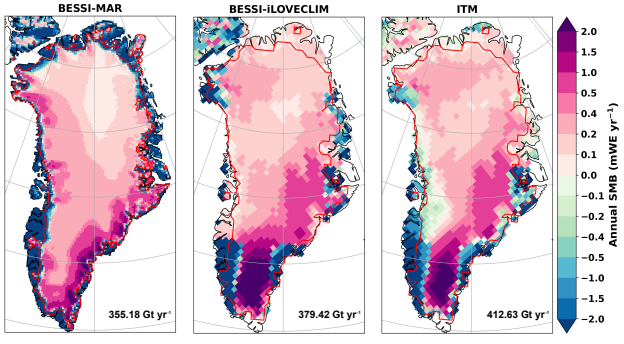

Figure 6. Comparison of annual mean SMB (in mWE yr^{-1}) between BESSI with different forcings: MAR and *i*LOVECLIM, and ITM for Greenland Ice Sheet. The total SMB (in Gt yr^{-1}) integrated for the present-day ice sheet extent (red line) is also included.

To investigate the influences of the forcings on the BESSI model, we compare the annual mean SMB during 1979-2021 between BESSI-MAR and BESSI-*i*LOVECLIM (Fig. 6). The patterns of the simulated SMB follow the patterns of precipitation of the climate forcings (Fig. 5a). BESSI-MAR has smoother SMB simulation as the resolution of MAR is finer than *i*LOVECLIM, particularly 15km vs 40km. This helps the model to capture narrow ablation around the margin in the West and North of the ice sheet, which is absent from the result of BESSI-*i*LOVECLIM. BESSI-*i* LOVECLIM overestimates both ablation and accumulation in the South of the ice sheet due to the bias in the climate of the forcing. Particularly, the magnitude of the negative SMB is very high in BESSI-*i*LOVECLIM, which is a result of the model setup itself, as this is also observed in BESSI-MAR and MAR comparison (Fig. 2a). Due to such warmer and drier climate conditions, BESSI-*i*LOVECLIM has higher rates of melt and sublimation/evaporation than MAR (Table 2). Despite these discrepancies in the magnitude of SMB,

https://doi.org/10.5194/egusphere-2024-556
Preprint. Discussion started: 18 March 2024

Table 2. Annual mean total SMB and its elements of different simulation: BESSI-MAR, BESSI-*i*LOVECLIM and ITM of GrIS and AIS.

Mass (in Gt yr^{-1})	Greeland			Antarctica		
	BESSI-MAR	BESSI-*i*LOVECLIM	ITM	BESSI-MAR	BESSI-*i*LOVECLIM	ITM
Total precipitation	702.85	923.00	923.00	2918.97	2184.01	2184.01
Melt	337.91	443.54	510.36	49.43	137.28	132.42
Refreezing	71.7	41.90	-	41.15	51.52	-
Runoff	306.75	476.87	-	18.59	138.91	-
Sublimation/Evaporation	40.92	66.70	-	94.57	201.69	-
SMB	355.18	379.43	412.63	2805.81	1843.45	2051.59

the patterns of SMB for both cases, overall, are quite similar. Also, the value of the total SMB from the two forcings is in the same range with around 20 Gt yr^{-1} difference.

In the same figure, we also compare BESSI with the current SMB scheme *i*LOVECLIM climate – ITM to gain insight into the behavior of the two models. A noticeable difference with reference to BESSI-*i*LOVECLIM is that the negative SMB zone around the West margin of the ice sheet is present and expands deep into the center (Fig. 6), which can possibly be a result of the temperature patterns (Fig. 5b). This indicates that ITM in this work overestimates the ablation zone, leading to excessive melt simulation with nearly 100 Gt yr^{-1} higher than BESSI-*i*LOVECLIM (Table 2). On the other hand, the low accumulation zone in the center North of the ice sheet related to sublimation/evaporation is not as clear as shown in BESSI-*i*LOVECLIM as ITM simulates only melt. Both models, unlike BESSI-MAR, have accumulation outside the ice sheet mask, possibly due to the native T21 grid of *i*LOVECLIM. Neglecting other processes besides melt, ITM obtains a higher total SMB value than BESSI even with a much larger ablation zone estimation (about 413 Gt yr^{-1} compared to 379 Gt yr^{-1}).

Antarctica

For AIS, the climate simulated by *i*LOVECLIM is not as wet as that of MAR, with a lower annual mean total precipitation value (Table 2). The bias in *i*LOVECLIM is consistent for both ice sheets in terms of temperature and humidity as similar patterns are observed for Antarctica (Fig. 7). Particularly, relative humidity in *i*LOVECLIM is much lower than in MAR, with a value of around 25%, resulting in an unrealistically dry climate (Fig. 7c).

A comparison of the annual mean SMB value of three different simulations, namely BESSI-MAR, BESSI-*i*LOVECLIM, and ITM for Antarctica, is illustrated in Fig. 8. A noticeably large ablation zone located in the center West and some parts of the East of the ice sheet in BESSI-*i*LOVECLIM that are not present in BESSI-MAR or even ITM is a result of very low humidity (Fig. 7c). This bias leads to unrealistic sublimation/evaporation simulation by BESSI-*i*LOVECLIM which is two times more than BESSI-MAR (around 202 Gt yr^{-1} compared to 95 Gt yr^{-1}). As the downscaling is only carried out for land grid boxes and due to T21 grid size, some parts of the ice sheet margins in BESSI-*i*LOVECLIM simulation are missing, for example, the

https://doi.org/10.5194/egusphere-2024-556
Preprint. Discussion started: 18 March 2024

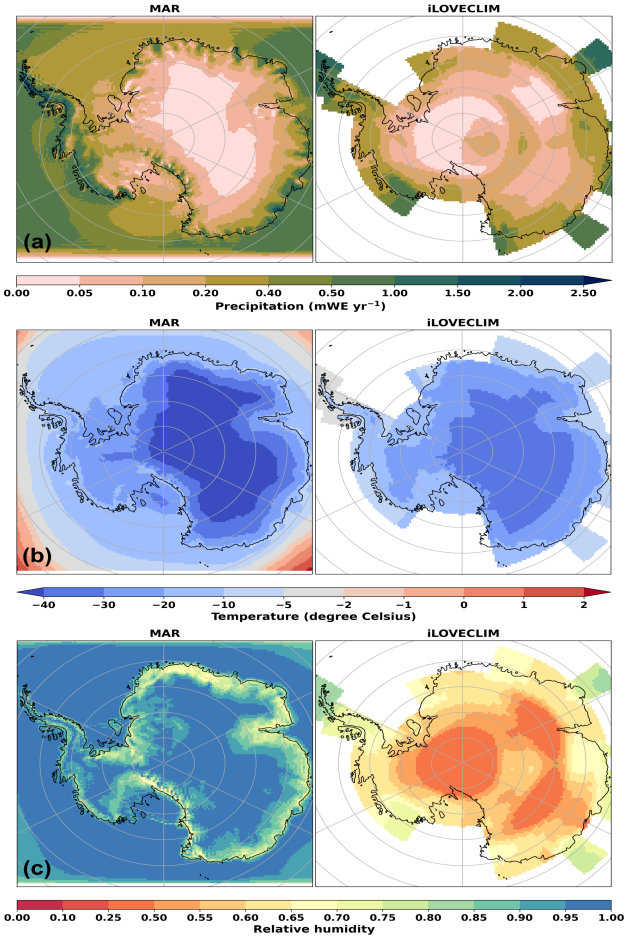

Figure 7. Annual mean value of climate variables including (**a**) precipitation (in mWE yr^{-1}), (**b**) near-surface temperature (in degree Celsius) and (**c**) relative humidity of MAR and *i*LOVECLIM for Antarctica Ice Sheet.

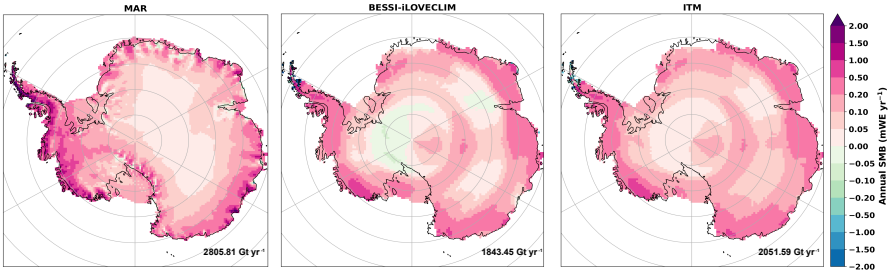

Figure 8. Comparison of annual mean SMB (in mWE yr^{-1}) between BESSI with different forcings: MAR and *i*LOVECLIM, and ITM for Antarctica Ice Sheet. The total SMB (in Gt yr^{-1}) integrated for the present-day ice sheet extent is also included.

https://doi.org/10.5194/egusphere-2024-556
Preprint. Discussion started: 18 March 2024

North of AIS (Fig. 8). The gap between BESSI forced by two different forcings is more than 1000 Gt yr^{-1}, around 34%, much higher than in Greenland (about 6.8%) due to lower precipitation but higher melts and excessive sublimation/evaporation. The melt estimated by ITM for AIS is slightly lower than BESSI-*i*LOVECLIM (around 132 and 137 Gt yr^{-1}, respectively), which is different from GrIS simulation due to a colder climate. Compared to ITM, BESSI-*i*LOVECLIM again has a lower annual mean total SMB value with a difference of around 200 Gt yr^{-1} due to unrealistic sublimation/evaporation estimation.

3.2.2 LIG transient simulations with BESSI forced by *i*LOVECLIM

To study the evolution of SMB during LIG, we present the temporal variation of the external forcings, the annual mean total SMB, and its sub-processes simulated by BESSI-*i*LOVECLIM for both ice sheets in Fig. 9. The rise of summer insolation in the North and the carbon dioxide concentration during the beginning of the LIG (Fig. 9a) induce an increase in the melt rate of Greenland (Fig.9b). During the same period, runoff has a higher accelerated rate than melt, indicating both rain and melt are not well refreeze due to warm climate (Eq. (12)) . As the insolation starts to drop after 127 kaBP, runoff and melt also decrease. In the same figure, total precipitation is shown to be slightly increase during the peak of insolation, which is expected as the climate is getting warmer. Meanwhile, sublimation/evaporation remains stable throughout the period with a low magnitude as this process is not dominant for GrIS. Refreezing also remains in low value for this ice sheet, however, a slight increase during the peak of the LIG is observed in Fig. 9b. The total SMB, in this case, is mostly driven by runoff (melt): strongly decreases during the rise of summer insolation, and then recovers after 127 kaBP. The maximum change of total SMB during the LIG is more than 600 Gt yr^{-1}, around 170% less than the beginning of LIG (13 5kaBP) value.

Compared to Greenland, during the same period, the annual mean values of total SMB and its elements fluctuate less in Antarctica (Fig. 9c). Particularly, the biggest gap of the total SMB is about 250 Gt yr^{-1}, which is nearly 15% of the value of the first time slice (135 kaBP), which is much lower than GrIS. Also, the magnitude of the simulated annual mean total SMB during the LIG is quite low for Antarctica if we consider the value of BESSI-MAR in the present-day climate. From the results of Sect. 3.2.1, the total SMB for Antarctica simulated by BESSI-*i*LOVECLIM might be around 1000 Gt yr^{-1} lower than BESSI-MAR if we consider the difference between two forcings is constant with time. During the LIG, even though the insolation at the South Pole decreases (Fig. 9a), AIS still experiences an increase in the melt (Fig. 9c). This is a result of a warmer climate which results in higher global mean temperature. The sublimation is more dominant in AIS than in GrIS because of a much drier climate. Even though the sublimation is impacted by iLOVECLIM biases, no temporal change of this flux is simulated by the model. This suggests that the influences of the bias in the humidity of *i*LOVECLIM is constant. Due to this and the low value of runoff, for this ice sheet, the variation of the total SMB follows the pattern of the total precipitation. It slightly increases during the peak of summer insolation in the North as a warmer climate induces more precipitation.

By plotting the total SMB differences between the Last Interglacial and the pre-industrial periods simulated by the same model, we investigate the magnitude of SMB variation for both BESSI-*i*LOVECLIM and ITM (Fig. 10). Figure 10a shows that, for Greenland, the gap between the two models widens during the peak of the LIG. This indicates the overestimation of melt in ITM compared to BESSI forced by the same climate conditions (Supplementary Fig. S2a), consistent with Fig. 6. When the temperature drops at the end of the LIG, ITM has slightly higher SMB differences than BESSI-*i*LOVECLIM. In

https://doi.org/10.5194/egusphere-2024-556
Preprint. Discussion started: 18 March 2024

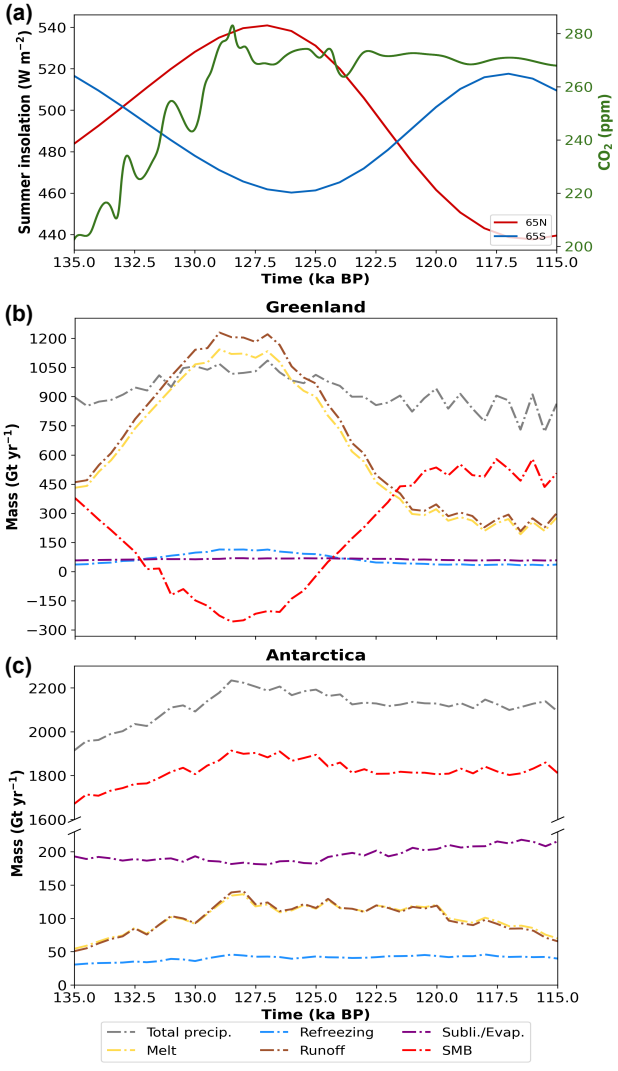

Figure 9. (**a**) Temporal variation of external forcings during the LIG: summer insolation of 65° N and 65° S (Berger, 1978) as well as the carbon dioxide concentration (in ppm) (Lüthi et al., 2008). (**b**) Temporal variation of the annual mean total SMB and its elements integrated on the present-day ice sheet extent of BESSI-*i*LOVECLIM (in Gt yr^{-1}) during LIG for Greenland. (**c**) Same as (**b**) but for Antarctica.

other words, when the climate is colder during the end of the LIG, ITM has a higher SMB rate compared to its pre-industrial simulation. This suggests that ITM displays a large sensitivity to temperature change. For Antarctica, the discrepancies between
360 ITM and BESSI as we compared the value of LIG and pre-industrial are less significant than in Greenland (Fig. 10b), as the change of total SMB in this region is insignificant. As Fig. 9c indicates that sublimation/evaporation is almost constant during the LIG, the gap between ITM and BESSI in Fig. 10b can only be explained by the difference in melt simulation. In contrast to BESSI-*i*LOVECLIM results, the melt rate in ITM simulation is quite stable (Supplementary Fig. S2b). This can be explained

https://doi.org/10.5194/egusphere-2024-556
Preprint. Discussion started: 18 March 2024

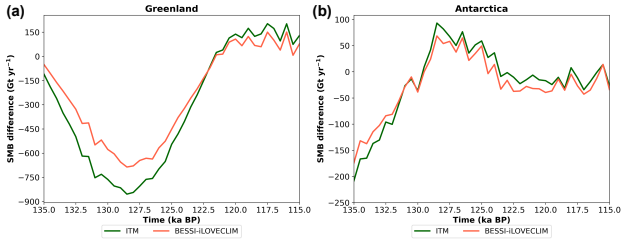

Figure 10. Comparison of BESSI-*i*LOVECLIM and ITM in terms of the annual mean total SMB differences (in Gt yr^{-1}) between LIG and pre-industrial for (**a**) Greenland and (**b**) Antarctica.

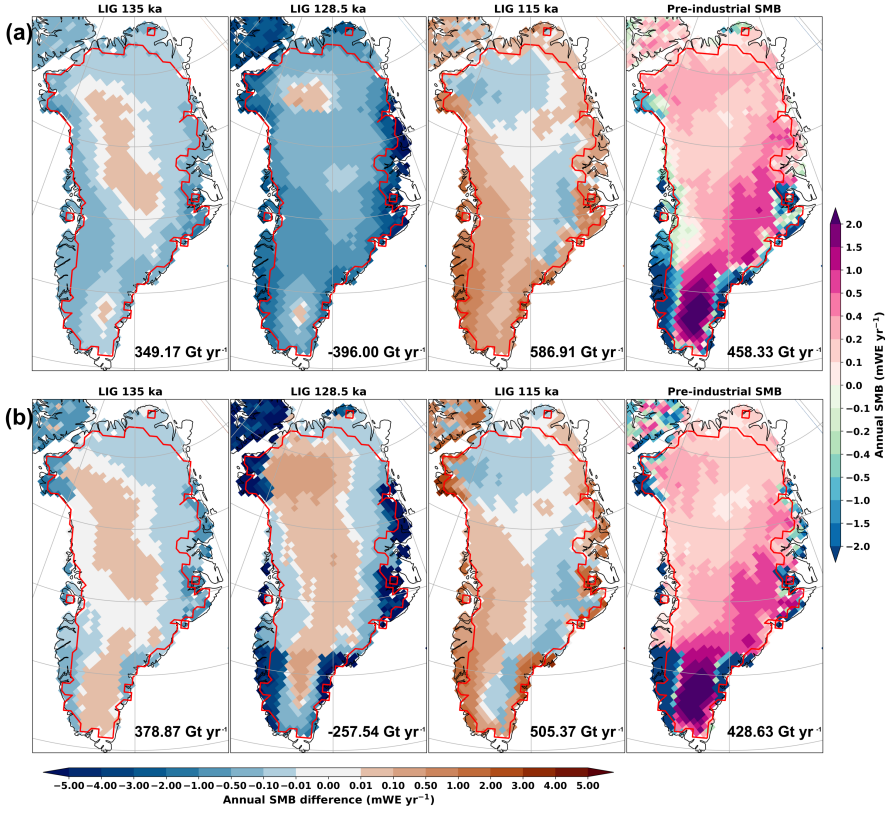

Figure 11. Annual mean SMB anomalies (in Gt yr^{-1}) between several LIG time slices (135, 128.5 and 115 kaBP) and the pre-industrial simulation of (**a**) ITM and (**b**) BESSI-*i*LOVECLIM for Greenland Ice Sheet. The absolute annual SMB value of PI and the total SMB (in Gt yr^{-1}) integrated for the present-day ice sheet extent (red line) of each simulation are also included.

that, since the climate of AIS is not as warm as GrIS, the sensitivity of ITM to the change of temperature is limited for this ice sheet. Also, albedo feedback is not taken into account in parameterizations such as ITM, which could also be the reason behind the difference in the simulation of melt between the two models.

https://doi.org/10.5194/egusphere-2024-556
Preprint. Discussion started: 18 March 2024

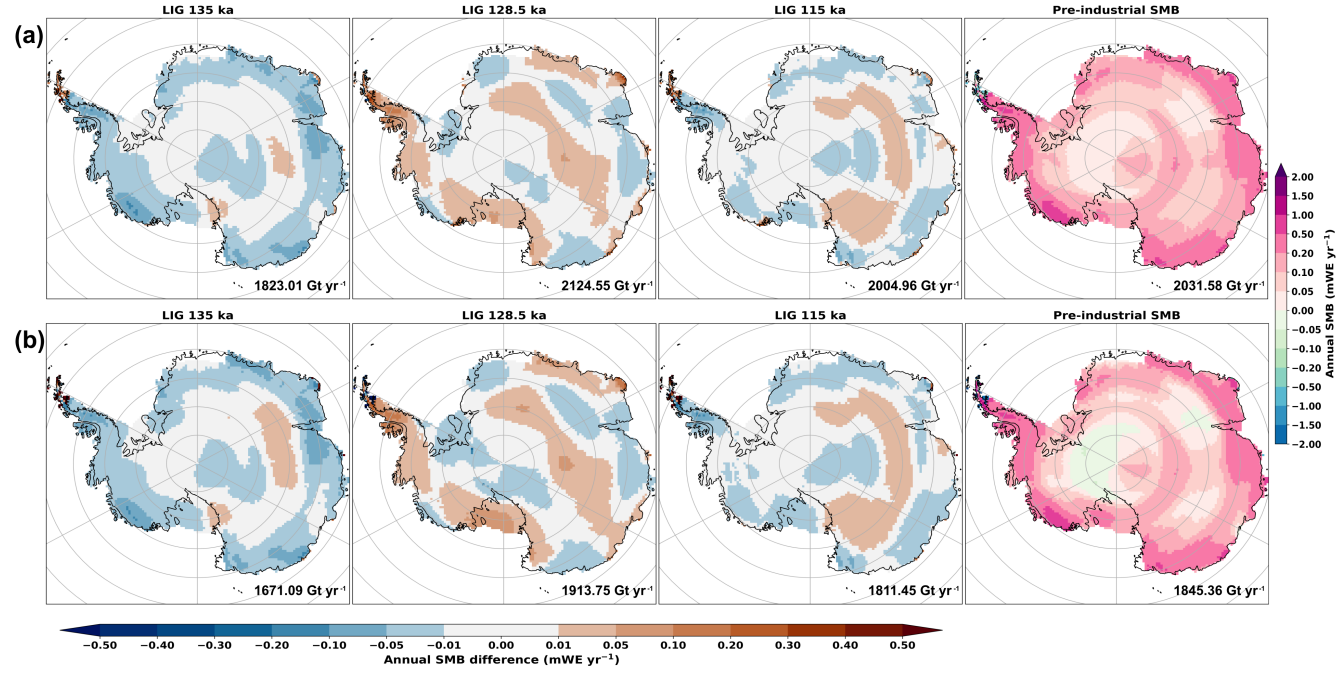

Figure 12. Annual mean SMB anomalies (in Gt yr^{-1}) between several LIG time slices (135, 128.5 and 115 kaBP) and the pre-industrial simulation of (**a**) ITM and (**b**) BESSI-*i*LOVECLIM for Antarctica Ice Sheet. The absolute annual SMB value of PI and the total SMB (in Gt yr^{-1}) integrated for the present-day ice sheet extent of each simulation are also included.

The patterns of the annual mean SMB differences between LIG and PI of ITM and BESSI-*i*LOVECLIM for GrIS are shown in Fig. 11. In this figure, we select three different time slices from the LIG simulation: the first (135 kaBP), the peak of the deglaciation (128.5 kaBP) and the last (115 kaBP) to further investigate the differences between the two different SMB schemes. The pre-industrial annual mean SMB of the two models is quite similar to the present-day value (Fig. 6). For the LIG, the two models display similar patterns for the first and the last time slices. Particularly, in the beginning of the LIG, for the two models, positive SMB differences can be seen in the inner part of the ice sheet as there is more precipitation. Meanwhile, SMB rates around the margin are lower than the pre-industrial value since the melting process is accelerated due to warmer climate conditions. This SMB trend is enhanced during the peak of deglaciation (128.5 kaBP). In the simulation of BESSI-*i*LOVECLIM, the magnitude of the negative differences around the margin is very high compared to ITM, which is due to the model itself, as mentioned before (Fig. 2 and Fig. 6). On the other hand, for the same time slice, the number of grid boxes with a higher SMB rate than the pre-industrial value in BESSI-*i*LOVECLIM simulation is much higher than that of ITM. This results from overestimating ablation zones in ITM (Supplementary Fig. S3a). BESSI-*i*LOVECLIM displays a very extreme value for the negative SMB rate; however, the spreading of ablation zones in its simulation is more restricted (Supplementary Fig. S3b). Then at the end of the LIG, both models simulate higher SMB rates around the margins as colder climate accelerates accumulation.

https://doi.org/10.5194/egusphere-2024-556
Preprint. Discussion started: 18 March 2024

Similar to GrIS, for AIS, we also investigate the patterns of the annual mean SMB differences between several time slices of LIG and PI in the simulations of ITM and BESSI-*i*LOVECLIM (Fig. 12). Again, the pre-industrial annual mean SMB of the two models is consistent to the present-day results (Fig. 8). However, contrary to the GrIS, fig. 12 suggests not much difference in the SMB value between the LIG and PI as well as between the two models for AIS. This is consistent with Fig. 10b, as the magnitude of the differences is very low compared to that of the absolute SMB value (Supplementary Fig. S4).

4 Discussion

In this work, we assess the feasibility of replacing a parameterization scheme (ITM) with a physical-based surface energy balance model (BESSI) to provide a more physical SMB approach for the *i*LOVECLIM model framework with a view to simulating the change of ice sheet in the past.

The snow model - BESSI shows good performance in the calibration/validation with MAR under the present-day climate. Highlighting the model's ability to simulate different climates faithfully, the first-ever simulation for Antarctica (without re-tuning) is in good agreement with MAR, which is more complex and has been intensively used to study this ice sheet. The version used here has been improved with the inclusion of turbulent latent heat flux, albedo aging scheme, and more input fields instead of parameterizations. These improvements enhance the model's capacity to simulate different SMB main components as more processes are taken into account. However, the issue related to the strong underestimation of refreezing (Plach et al., 2018; Born et al., 2019) still remains (Fig. 3). Lowering the time step of the model from daily to hourly might solve this problem, as the current model's large time step (daily) possibly neglects the diurnal cycle of temperature (Krebs-Kanzow et al., 2018). On the other hand, the ablation simulated by BESSI is underestimated in extent but mostly overestimated in magnitude. Particularly, the narrow ablation zone in the south-western of GrIS is underestimated in BESSI-MAR, compared to MAR (Fig. 2), which is also reported in Fettweis et al. (2020). However, due to the compensation of melt and refreezing, the results of the snow model are in good range with respect to MAR.

For long-term simulations in paleo studies, BESSI has proved to be able to provide reliable data in a short time as it has a physical model setup and is computationally inexpensive. Particularly, in this work, BESSI-*i*LOVECLIM simulates well the SMB evolution during the LIG, following the change of the orbital configuration and carbon dioxide concentration. The snow model gives details not only about the SMB but also its major processes at a much cheaper cost than the energy surface schemes embedded in regional climate models.

Compared to the existing SMB scheme of *i*LOVECLIM - ITM, BESSI simulates less melt with more complexity in model setup. Here we used the ITM version without any modification to adapt to the climate of *i*LOVECLIM to provide a robust comparison between BESSI and ITM. ITM is a simple parameterization that strongly depends on its empirical parameters and temperature (Eq. (15)). A small change in one of its parameters (such as c) can influence the melt rate significantly for the region where this process is dominant. For example, we use c = -25 W m^{-2} to obtain the results in Sect. 3.2.2. For a lower value of c, such as -40 W m^{-2}, ITM produces less melt in GrIS, while in AIS, there is no difference in the SMB results (Fig. B1). It is hard to draw a conclusion about the comparison of the two models' performance. However, it is clear that results from BESSI

https://doi.org/10.5194/egusphere-2024-556
Preprint. Discussion started: 18 March 2024

are more physically constrained and, therefore, are more reliable. Hence, replacing ITM with BESSI to provide SMB to the ice sheet model GRISLI in *i*LOVECLIM framework is possible and can help to produce more physical results. However, this might also add more sources of uncertainties to the model as BESSI needs more input fields than ITM. Particularly, as ITM only simulates melt, the bias from *i*LOVECLIM climate related to humidity in the AIS region does not influence ITM as much as in the BESSI case. For paleoclimate studies, using a physical-based model like BESSI helps to take into account the change of other factors besides temperature, such as insolation or humidity, and important processes like albedo feedback, which a simple parameterization scheme cannot capture well.

As any climate model, *i*LOVECLIM displays some biases which can be locally dominant (Heinemann et al., 2014). In this work, we investigate three climate variables: precipitation, near-surface temperature, and relative humidity to document the bias of *i*LOVECLIM in two polar ice sheet regions. The results of Sect. 3.2.1 indicates that the climate in *i*LOVECLIM, compared to MAR, is warmer and less humid for both ice sheets, with a very low humidity for AIS. These biases strongly impact the performance of the snow model, resulting in overestimation of melts and excessive sublimation/evaporation rate. Therefore, the simulated SMB does not agree with MAR, particularly for AIS. This is unavoidable as *i*LOVECLIM is much less complex than state-of-the-art regional climate models such as MAR. However, transient LIG climate forcings can be obtained with much more favorable computational efficiency thanks to such a simple model setup. Carrying out bias correction for some crucial atmospheric variables in *i*LOVECLIM can tackle the problems of unrealistic climate patterns, leading to a better performance of the snow model and ITM in the SMB simulation. For example, with a simple delta method to correct the bias in *i*LOVECLIM climate (see Appendix B), results of BESSI-*i*LOVECLIM are improved for the present-day (Fig. B2) as well as the LIG (Fig. B1). With a more sophisticated bias correction method, the results can be further improved.

5 Conclusions

This work examines the feasibility of switching the SMB scheme of the Earth system model of intermediate complexity *i*LOVECLIM from a simple parameterization (ITM) to a physical-based surface energy balance model (BESSI) for the purpose of improving the simulation of ice sheet-climate interaction. BESSI exhibits good performance in the validation in the present-day period by MAR, a state-of-the-art regional climate model that includes a full physical energy mass transfer scheme of the surface, for two very different ice sheet climate conditions: GrIS and AIS. Then, *i*LOVECLIM is used as BESSI's forcing for a paleoclimate simulation: the Last Interglacial period. *i*LOVECLIM displays a large-scale climate change consistent with the forcings that translate to SMB evolution in agreement with previous modeling work. Switching from MAR to *i*LOVECLIM highlights the strong influence of climate forcing on the simulation of snow and SMB evolution. In particular, *i*LOVECLIM presents important bias that leads to some large misrepresentation of present-day SMB for both Greenland and Antarctic ice sheets. These unrealistic climate patterns hamper the performance of BESSI, posing the need for bias correction of the climate fields in *i*LOVECLIM. The comparison between BESSI forced by *i*LOVECLIM and ITM during the Last Interglacial indicates a strong sensitivity of ITM to the temperature. The current SMB scheme of *i*LOVECLIM also shows a strong dependence on the value empirical parameters, which means it can easily be tuned, not physically constrained. The results suggest BESSI can

https://doi.org/10.5194/egusphere-2024-556
Preprint. Discussion started: 18 March 2024

be used to replace ITM in *i*LOVECLIM as this snow model maintains the low computational cost of the parameterization SMB scheme whilst providing more reliable results.

https://doi.org/10.5194/egusphere-2024-556
Preprint. Discussion started: 18 March 2024

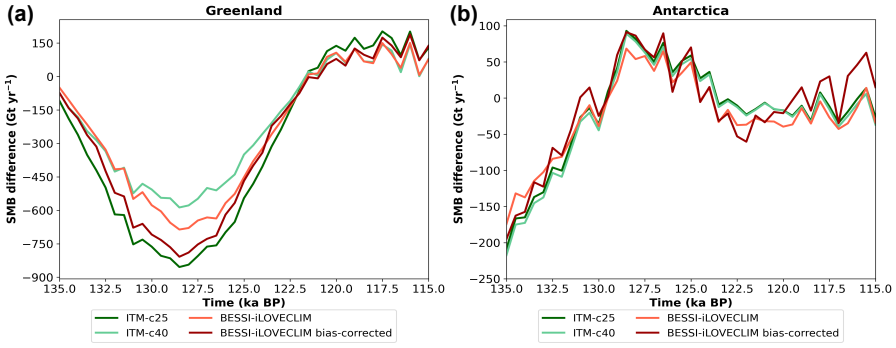

Figure B1. Comparison of ITM of different value of parameter c and BESSI with original and bias-corrected *i*LOVECLIM in terms of the annual mean total SMB anomalies (in Gt yr^{-1}) between LIG and pre-industrial for (**a**) Greenland and (**b**) Antarctica.

Appendix A: Evaluation metrics for BESSI-MAR and MAR comparison

The goodness-of-fit metrics used to evaluate BESSI performance for the present-day climate condition are presented in the following. The coefficient of determination R^2 is calculated as:

$$R^2 = 1 - \frac{\sum_i^n (X_{BESSI_i} - X_{MAR_i})^2}{\sum_i^n (X_{MAR_i} - \overline{X_{MAR}})^2} \tag{A1}$$

in which $(X_{BESSI_i} - X_{MAR_i})$ is the difference between the climatological annual mean value of the same variable of two models for the grid cell i. $\overline{X_{MAR}}$ indicates the spatial mean value of MAR of 43-year-mean result.

The Root Mean Squared Errors (RMSE) is defined as:

$$RMSE = \sqrt{\frac{1}{n}\sum_i^n (X_{BESSI_i} - X_{MAR_i})^2} \tag{A2}$$

Here, n is the total number of the grid points of each ice sheet domain: 7,667 for GrIS and 11,217 for AIS, which is also the case for Eq.A1.

For a better intercomparison of different variables, we used Normalised RMSE, defined as:

$$NRMSE = \frac{1}{\sigma_{MAR}} \sqrt{\frac{1}{n}\sum_i^n (X_{BESSI_i} - X_{MAR_i})^2} \tag{A3}$$

with σ_{MAR} is the standard deviation of MAR model climatological annual mean output.

https://doi.org/10.5194/egusphere-2024-556
Preprint. Discussion started: 18 March 2024

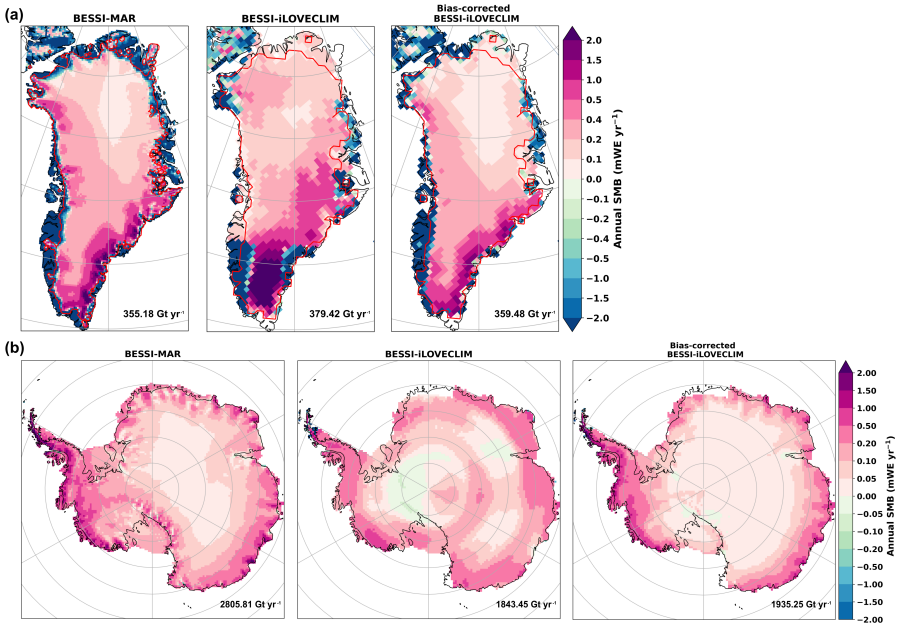

Figure B2. Comparison of BESSI-*i*LOVECLIM and ITM of different value of parameter c in terms of the annual mean total SMB anomalies (in Gt yr^{-1}) between LIG and pre-industrial for(**a**) Greenland and (**b**) Antarctica.

Appendix B: Additional plots

B1 ITM with c = -40 W m^{-2}

To illustrate the dependence of ITM on its empirical parameters, we carry out a LIG simulation with a lower value of c parameter in Eq. (15) by using c = -40 W m^{-2}. The results are presented in Fig. B1. As expected, ITM with a lower c value simulates less melt for regions with large temperature changes during the LIG (GrIS).

B2 Bias correction method for *i*LOVECLIM

To investigate the influence of bias-corrected *i*LOVECLIM on BESSI's performance, we use the delta method to correct the bias in *i*LOVECLIM by using ERA5 (Muñoz-Sabater et al., 2021), a reanalysis climate data, as reference.

Input for BESSI includes near-surface temperature, precipitation, surface pressures, humidity, and short-/long-wave radiation in daily time steps. For temperature, the bias-corrected data is obtained as follows:

$$T'_{iLC} = T_{iLC} + (\overline{T_{ERA5}} - \overline{T_{iLC}}) \tag{B1}$$

in which, T'_{iLC} is the bias-corrected daily temperature of *i*LOVECLIM, T_{iLC} is the origin daily output of *i*LOVECLIM, $(\overline{T_{ERA5}} - \overline{T_{iLC}})$ is the differences in the daily climatological mean temperature of the period 1979-2021 between ERA5 and *i*LOVECLIM.

https://doi.org/10.5194/egusphere-2024-556
Preprint. Discussion started: 18 March 2024

For other input variables, the bias correction is carried out as:

$$X'_{iLC} = X_{iLC} \times \frac{\overline{X_{ERA5}}}{\overline{X_{iLC}}} \tag{B2}$$

in which, X'_{iLC} is the bias-corrected daily data of *i*LOVECLIM, X_{iLC} is the origin daily output of *i*LOVECLIM, $\overline{X_{ERA5}}$ and $\overline{X_{iLC}}$ is the daily climatological mean data of the period 1979-2021 correspondent to the reference (ERA5) and *i*LOVECLIM. In order to avoid extreme value, we set a threshold for the ratio $\frac{\overline{X_{ERA5}}}{\overline{X_{iLC}}}$ to be in the range 0.1-10.0.

We present the result of the bias correction for present-day climate in Fig. B2. For the Greenland ice sheet (Fig. B2a), bias-corrected BESSI-*i*LOVECLIM displays better SMB patterns than the original version with BESSI-MAR as a reference. Similarly, the unrealistic negative SMB in the center of the Antarctic ice sheet is also removed with the bias correction (Fig. B2a).

Assuming the biases are constant with time, we run bias-corrected BESSI-*i*LOVECLIM for the LIG with the same bias-corrected factors obtained from present-day simulations. The results are presented in Fig. B1 (also in Supplementary Fig. S5). Compared to the pre-industrial simulation of the same model, bias-corrected BESSI-*i*LOVECLIM simulates more melt than the origin model version during the LIG in GrIS. For AIS, not much differences are observed between the two versions of BESSI-*i*LOVECLIM.

https://doi.org/10.5194/egusphere-2024-556
Preprint. Discussion started: 18 March 2024

Data availability. Archiving of source data of the figures presented in the main text of the manuscript is underway. Data will be made publicly available upon publication of the manuscript on the Zenodo repository with digital object identifier 10.xxxx/zenodo.xxxxxxx. They are temporarily available for review purposes upon request.

Code availability. BESSI version used in this work will be made publicly available upon publication of the manuscript on the Zenodo repository with digital object identifier 10.xxxx/zenodo.xxxxxxx.

Author contributions. TKDH and AQ designed the study with contributions from CD and DMR. AB provided the source code of the BESSI model. All authors contributed to the analysis of the results. TKDH performed the simulations and wrote the manuscript with comments from AQ, CD, AB and DMR.

Competing interests. The authors declare that they have no conflict of interest.

Acknowledgements. Thi-Khanh-Dieu Hoang was supported by the CEA NUMERICS program, which has received funding from the European Union's Horizon 2020 research and innovation program under the Marie Sklodowska-Curie grant agreement No 800945. The authors would like to thank Xavier Fettweis, Charles Amory and Cécile Agosta for providing the data of MAR for GrIS and AIS. We also acknowledge the Institut Pierre Simon Laplace for hosting the iLOVECLIM model code under the LUDUS framework project (http://forge.ipsl.jussieu.fr/ludus last access: 23 February 2024).

https://doi.org/10.5194/egusphere-2024-556
Preprint. Discussion started: 18 March 2024

References

Agosta, C., Amory, C., Kittel, C., Orsi, A., Favier, V., Gallée, H., van den Broeke, M. R., Lenaerts, J. T. M., van Wessem, J. M., van de Berg, W. J., and Fettweis, X.: Estimation of the Antarctic surface mass balance using the regional climate model MAR (1979–2015) and identification of dominant processes, The Cryosphere, 13, 281–296, https://doi.org/10.5194/tc-13-281-2019, publisher: Copernicus GmbH, 2019.

Bauer, E. and Ganopolski, A.: Comparison of surface mass balance of ice sheets simulated by positive-degree-day method and energy balance approach, Climate of the Past, 13, 819–832, https://doi.org/10.5194/cp-13-819-2017, publisher: Copernicus GmbH, 2017.

Berger, A.: Long-Term Variations of Daily Insolation and Quaternary Climatic Changes, Journal of the Atmospheric Sciences, 35, 2362–2367, https://doi.org/10.1175/1520-0469(1978)035<2362:LTVODI>2.0.CO;2, publisher: American Meteorological Society Section: Journal of the Atmospheric Sciences, 1978.

Born, A. and Nisancioglu, K. H.: Melting of Northern Greenland during the last interglaciation, The Cryosphere, 6, 1239–1250, https://doi.org/10.5194/tc-6-1239-2012, publisher: Copernicus GmbH, 2012.

Born, A., Imhof, M. A., and Stocker, T. F.: An efficient surface energy–mass balance model for snow and ice, The Cryosphere, 13, 1529–1546, https://doi.org/10.5194/tc-13-1529-2019, publisher: Copernicus GmbH, 2019.

Bouttes, N., Swingedouw, D., Roche, D. M., Sanchez-Goni, M. F., and Crosta, X.: Response of the carbon cycle in an intermediate complexity model to the different climate configurations of the last nine interglacials, Climate of the Past, 14, 239–253, https://doi.org/10.5194/cp-14-239-2018, publisher: Copernicus GmbH, 2018.

Bouttes, N., Lhardy, F., Quiquet, A., Paillard, D., Goosse, H., and Roche, D. M.: Deglacial climate changes as forced by different ice sheet reconstructions, Climate of the Past, 19, 1027–1042, https://doi.org/10.5194/cp-19-1027-2023, publisher: Copernicus GmbH, 2023.

Bradley, S., Siddall, M., Milne, G., Masson-Delmotte, V., and Wolff, E.: Combining ice core records and ice sheet models to explore the evolution of the East Antarctic Ice sheet during the Last Interglacial period, Global and Planetary Change, 100, 278–290, https://doi.org/10.1016/j.gloplacha.2012.11.002, 2013.

Brovkin, V., Ganopolski, A., and Svirezhev, Y.: A continuous climate-vegetation classification for use in climate-biosphere studies, Ecological Modelling, 101, 251–261, https://doi.org/10.1016/S0304-3800(97)00049-5, 1997.

Claussen, M., Mysak, L., Weaver, A., Crucifix, M., Fichefet, T., Loutre, M.-F., Weber, S., Alcamo, J., Alexeev, V., Berger, A., Calov, R., Ganopolski, A., Goosse, H., Lohmann, G., Lunkeit, F., Mokhov, I., Petoukhov, V., Stone, P., and Wang, Z.: Earth system models of intermediate complexity: closing the gap in the spectrum of climate system models, Climate Dynamics, 18, 579–586, https://doi.org/10.1007/s00382-001-0200-1, 2002.

Dee, D. P., Uppala, S. M., Simmons, A. J., Berrisford, P., Poli, P., Kobayashi, S., Andrae, U., Balmaseda, M. A., Balsamo, G., Bauer, P., Bechtold, P., Beljaars, A. C. M., van de Berg, L., Bidlot, J., Bormann, N., Delsol, C., Dragani, R., Fuentes, M., Geer, A. J., Haimberger, L., Healy, S. B., Hersbach, H., Hólm, E. V., Isaksen, L., Kållberg, P., Köhler, M., Matricardi, M., McNally, A. P., Monge-Sanz, B. M., Morcrette, J.-J., Park, B.-K., Peubey, C., de Rosnay, P., Tavolato, C., Thépaut, J.-N., and Vitart, F.: The ERA-Interim reanalysis: configuration and performance of the data assimilation system, Quarterly Journal of the Royal Meteorological Society, 137, 553–597, https://doi.org/10.1002/qj.828, _eprint: https://onlinelibrary.wiley.com/doi/pdf/10.1002/qj.828, 2011.

Dutton, A. and Lambeck, K.: Ice Volume and Sea Level During the Last Interglacial, Science, 337, 216–219, https://doi.org/10.1126/science.1205749, 2012.

https://doi.org/10.5194/egusphere-2024-556
Preprint. Discussion started: 18 March 2024

Dutton, A., Carlson, A. E., Long, A. J., Milne, G. A., Clark, P. U., DeConto, R., Horton, B. P., Rahmstorf, S., and Raymo, M. E.: Sea-level rise due to polar ice-sheet mass loss during past warm periods, Science, 349, aaa4019, https://doi.org/10.1126/science.aaa4019, 2015.

Dyer, B., Austermann, J., D'Andrea, W. J., Creel, R. C., Sandstrom, M. R., Cashman, M., Rovere, A., and Raymo, M. E.: Sea-level trends across The Bahamas constrain peak last interglacial ice melt, Proceedings of the National Academy of Sciences, 118, e2026839 118, https://doi.org/10.1073/pnas.2026839118, publisher: Proceedings of the National Academy of Sciences, 2021.

Eby, M., Weaver, A. J., Alexander, K., Zickfeld, K., Abe-Ouchi, A., Cimatoribus, A. A., Crespin, E., Drijfhout, S. S., Edwards, N. R., Eliseev, A. V., Feulner, G., Fichefet, T., Forest, C. E., Goosse, H., Holden, P. B., Joos, F., Kawamiya, M., Kicklighter, D., Kienert, H., Matsumoto, K., Mokhov, I. I., Monier, E., Olsen, S. M., Pedersen, J. O. P., Perrette, M., Philippon-Berthier, G., Ridgwell, A., Schlosser, A., Schneider von Deimling, T., Shaffer, G., Smith, R. S., Spahni, R., Sokolov, A. P., Steinacher, M., Tachiiri, K., Tokos, K., Yoshimori, M., Zeng, N., and Zhao, F.: Historical and idealized climate model experiments: an intercomparison of Earth system models of intermediate complexity, Climate of the Past, 9, 1111–1140, https://doi.org/10.5194/cp-9-1111-2013, publisher: Copernicus GmbH, 2013.

Ettema, J., van den Broeke, M. R., van Meijgaard, E., van de Berg, W. J., Bamber, J. L., Box, J. E., and Bales, R. C.: Higher surface mass balance of the Greenland ice sheet revealed by high-resolution climate modeling, Geophysical Research Letters, 36, https://doi.org/10.1029/2009GL038110, _eprint: https://onlinelibrary.wiley.com/doi/pdf/10.1029/2009GL038110, 2009.

Fettweis, X.: Reconstruction of the 1979–2006 Greenland ice sheet surface mass balance using the regional climate model MAR, The Cryosphere, 1, 21–40, https://doi.org/10.5194/tc-1-21-2007, publisher: Copernicus GmbH, 2007.

Fettweis, X., Franco, B., Tedesco, M., van Angelen, J. H., Lenaerts, J. T. M., van den Broeke, M. R., and Gallée, H.: Estimating the Greenland ice sheet surface mass balance contribution to future sea level rise using the regional atmospheric climate model MAR, The Cryosphere, 7, 469–489, https://doi.org/10.5194/tc-7-469-2013, publisher: Copernicus GmbH, 2013.

Fettweis, X., Box, J. E., Agosta, C., Amory, C., Kittel, C., Lang, C., van As, D., Machguth, H., and Gallée, H.: Reconstructions of the 1900–2015 Greenland ice sheet surface mass balance using the regional climate MAR model, The Cryosphere, 11, 1015–1033, https://doi.org/10.5194/tc-11-1015-2017, publisher: Copernicus GmbH, 2017.

Fettweis, X., Hofer, S., Krebs-Kanzow, U., Amory, C., Aoki, T., Berends, C. J., Born, A., Box, J. E., Delhasse, A., Fujita, K., Gierz, P., Goelzer, H., Hanna, E., Hashimoto, A., Huybrechts, P., Kapsch, M.-L., King, M. D., Kittel, C., Lang, C., Langen, P. L., Lenaerts, J. T. M., Liston, G. E., Lohmann, G., Mernild, S. H., Mikolajewicz, U., Modali, K., Mottram, R. H., Niwano, M., Noël, B., Ryan, J. C., Smith, A., Streffing, J., Tedesco, M., van de Berg, W. J., van den Broeke, M., van de Wal, R. S. W., van Kampenhout, L., Wilton, D., Wouters, B., Ziemen, F., and Zolles, T.: GrSMBMIP: intercomparison of the modelled 1980–2012 surface mass balance over the Greenland Ice Sheet, The Cryosphere, 14, 3935–3958, https://doi.org/10.5194/tc-14-3935-2020, publisher: Copernicus GmbH, 2020.

Fischer, H., Meissner, K. J., Mix, A. C., Abram, N. J., Austermann, J., Brovkin, V., Capron, E., Colombaroli, D., Daniau, A.-L., Dyez, K. A., Felis, T., Finkelstein, S. A., Jaccard, S. L., McClymont, E. L., Rovere, A., Sutter, J., Wolff, E. W., Affolter, S., Bakker, P., Ballesteros-Cánovas, J. A., Barbante, C., Caley, T., Carlson, A. E., Churakova (Sidorova), O., Cortese, G., Cumming, B. F., Davis, B. A. S., de Vernal, A., Emile-Geay, J., Fritz, S. C., Gierz, P., Gottschalk, J., Holloway, M. D., Joos, F., Kucera, M., Loutre, M.-F., Lunt, D. J., Marcisz, K., Marlon, J. R., Martinez, P., Masson-Delmotte, V., Nehrbass-Ahles, C., Otto-Bliesner, B. L., Raible, C. C., Risebrobakken, B., Sánchez Goñi, M. F., Arrigo, J. S., Sarnthein, M., Sjolte, J., Stocker, T. F., Velasquez Alvárez, P. A., Tinner, W., Valdes, P. J., Vogel, H., Wanner, H., Yan, Q., Yu, Z., Ziegler, M., and Zhou, L.: Palaeoclimate constraints on the impact of 2 °C anthropogenic warming and beyond, Nature Geoscience, 11, 474–485, https://doi.org/10.1038/s41561-018-0146-0, number: 7 Publisher: Nature Publishing Group, 2018.

Goelzer, H., Huybrechts, P., Loutre, M.-F., and Fichefet, T.: Impact of ice sheet meltwater fluxes on the climate evolution at the onset of the Last Interglacial, Climate of the Past, 12, 1721–1737, https://doi.org/10.5194/cp-12-1721-2016, publisher: Copernicus GmbH, 2016a.

https://doi.org/10.5194/egusphere-2024-556
Preprint. Discussion started: 18 March 2024

Goelzer, H., Huybrechts, P., Loutre, M.-F., and Fichefet, T.: Last Interglacial climate and sea-level evolution from a coupled ice sheet–climate model, Climate of the Past, 12, 2195–2213, https://doi.org/10.5194/cp-12-2195-2016, publisher: Copernicus GmbH, 2016b.

Goosse, H. and Fichefet, T.: Importance of ice-ocean interactions for the global ocean circulation: A model study, Journal of Geophysical Research: Oceans, 104, 23 337–23 355, https://doi.org/10.1029/1999JC900215, _eprint: https://onlinelibrary.wiley.com/doi/pdf/10.1029/1999JC900215, 1999.

Goosse, H., Brovkin, V., Fichefet, T., Haarsma, R., Huybrechts, P., Jongma, J., Mouchet, A., Selten, F., Barriat, P.-Y., Campin, J.-M., Deleersnijder, E., Driesschaert, E., Goelzer, H., Janssens, I., Loutre, M.-F., Morales Maqueda, M. A., Opsteegh, T., Mathieu, P.-P., Munhoven, G., Pettersson, E. J., Renssen, H., Roche, D. M., Schaeffer, M., Tartinville, B., Timmermann, A., and Weber, S. L.: Description of the Earth system model of intermediate complexity LOVECLIM version 1.2, Geoscientific Model Development, 3, 603–633, https://doi.org/10.5194/gmd-3-603-2010, publisher: Copernicus GmbH, 2010.

Gregory, J. M., Browne, O. J. H., Payne, A. J., Ridley, J. K., and Rutt, I. C.: Modelling large-scale ice-sheet–climate interactions following glacial inception, Climate of the Past, 8, 1565–1580, https://doi.org/10.5194/cp-8-1565-2012, publisher: Copernicus GmbH, 2012.

Heinemann, M., Timmermann, A., Elison Timm, O., Saito, F., and Abe-Ouchi, A.: Deglacial ice sheet meltdown: orbital pacemaking and CO_2 effects, Climate of the Past, 10, 1567–1579, https://doi.org/10.5194/cp-10-1567-2014, publisher: Copernicus GmbH, 2014.

Holube, K. M., Zolles, T., and Born, A.: Sources of uncertainty in Greenland surface mass balance in the 21st century, The Cryosphere, 16, 315–331, https://doi.org/10.5194/tc-16-315-2022, publisher: Copernicus GmbH, 2022.

Kittel, C., Amory, C., Agosta, C., Jourdain, N. C., Hofer, S., Delhasse, A., Doutreloup, S., Huot, P.-V., Lang, C., Fichefet, T., and Fettweis, X.: Diverging future surface mass balance between the Antarctic ice shelves and grounded ice sheet, The Cryosphere, 15, 1215–1236, https://doi.org/10.5194/tc-15-1215-2021, publisher: Copernicus GmbH, 2021.

Kopp, R. E., Simons, F. J., Mitrovica, J. X., Maloof, A. C., and Oppenheimer, M.: A probabilistic assessment of sea level variations within the last interglacial stage, Geophysical Journal International, 193, 711–716, https://doi.org/10.1093/gji/ggt029, 2013.

Krebs-Kanzow, U., Gierz, P., and Lohmann, G.: Brief communication: An ice surface melt scheme including the diurnal cycle of solar radiation, The Cryosphere, 12, 3923–3930, https://doi.org/10.5194/tc-12-3923-2018, publisher: Copernicus GmbH, 2018.

Kukla, G. J., Bender, M. L., Beaulieu, J.-L. d., Bond, G., Broecker, W. S., Cleveringa, P., Gavin, J. E., Herbert, T. D., Imbrie, J., Jouzel, J., Keigwin, L. D., Knudsen, K.-L., McManus, J. F., Merkt, J., Muhs, D. R., Müller, H., Poore, R. Z., Porter, S. C., Seret, G., Shackleton, N. J., Turner, C., Tzedakis, P. C., and Winograd, I. J.: Last Interglacial Climates, Quaternary Research, 58, 2–13, https://doi.org/10.1006/qres.2001.2316, publisher: Cambridge University Press, 2002.

Landais, A., Masson-Delmotte, V., Capron, E., Langebroek, P. M., Bakker, P., Stone, E. J., Merz, N., Raible, C. C., Fischer, H., Orsi, A., Prié, F., Vinther, B., and Dahl-Jensen, D.: How warm was Greenland during the last interglacial period?, Climate of the Past, 12, 1933–1948, https://doi.org/10.5194/cp-12-1933-2016, publisher: Copernicus GmbH, 2016.

Lenaerts, J. T. M., Medley, B., van den Broeke, M. R., and Wouters, B.: Observing and Modeling Ice Sheet Surface Mass Balance, Reviews of Geophysics, 57, 376–420, https://doi.org/10.1029/2018RG000622, _eprint: https://onlinelibrary.wiley.com/doi/pdf/10.1029/2018RG000622, 2019.

Lhardy, F., Bouttes, N., Roche, D. M., Crosta, X., Waelbroeck, C., and Paillard, D.: Impact of Southern Ocean surface conditions on deep ocean circulation during the LGM: a model analysis, Climate of the Past, 17, 1139–1159, https://doi.org/10.5194/cp-17-1139-2021, publisher: Copernicus GmbH, 2021a.

Lhardy, F., Bouttes, N., Roche, D. M., Abe Ouchi, A., Chase, Z., Crichton, K. A., Ilyina, T., Ivanovic, R., Jochum, M., Kageyama, M., Kobayashi, H., Liu, B., Menviel, L., Muglia, J., Nuterman, R., Oka, A., Vettoretti, G., and Yamamoto, A.: A First Intercomparison of the

Simulated LGM Carbon Results Within PMIP-Carbon: Role of the Ocean Boundary Conditions, Paleoceanography and Paleoclimatology, 36, e2021PA004 302, https://doi.org/10.1029/2021PA004302, _eprint: https://onlinelibrary.wiley.com/doi/pdf/10.1029/2021PA004302, 2021b.

Liakka, J., Löfverström, M., and Colleoni, F.: The impact of the North American glacial topography on the evolution of the Eurasian ice sheet over the last glacial cycle, Climate of the Past, 12, 1225–1241, https://doi.org/10.5194/cp-12-1225-2016, publisher: Copernicus GmbH, 2016.

Lunt, D. J., Abe-Ouchi, A., Bakker, P., Berger, A., Braconnot, P., Charbit, S., Fischer, N., Herold, N., Jungclaus, J. H., Khon, V. C., Krebs-Kanzow, U., Langebroek, P. M., Lohmann, G., Nisancioglu, K. H., Otto-Bliesner, B. L., Park, W., Pfeiffer, M., Phipps, S. J., Prange, M., Rachmayani, R., Renssen, H., Rosenbloom, N., Schneider, B., Stone, E. J., Takahashi, K., Wei, W., Yin, Q., and Zhang, Z. S.: A multi-model assessment of last interglacial temperatures, Climate of the Past, 9, 699–717, https://doi.org/10.5194/cp-9-699-2013, publisher: Copernicus GmbH, 2013.

Lüthi, D., Le Floch, M., Bereiter, B., Blunier, T., Barnola, J.-M., Siegenthaler, U., Raynaud, D., Jouzel, J., Fischer, H., Kawamura, K., and Stocker, T. F.: High-resolution carbon dioxide concentration record 650,000–800,000 years before present, Nature, 453, 379–382, https://doi.org/10.1038/nature06949, number: 7193 Publisher: Nature Publishing Group, 2008.

Mankoff, K. D., Fettweis, X., Langen, P. L., Stendel, M., Kjeldsen, K. K., Karlsson, N. B., Noël, B., van den Broeke, M. R., Solgaard, A., Colgan, W., Box, J. E., Simonsen, S. B., King, M. D., Ahlstrøm, A. P., Andersen, S. B., and Fausto, R. S.: Greenland ice sheet mass balance from 1840 through next week, Earth System Science Data, 13, 5001–5025, https://doi.org/10.5194/essd-13-5001-2021, publisher: Copernicus GmbH, 2021.

Muñoz-Sabater, J., Dutra, E., Agustí-Panareda, A., Albergel, C., Arduini, G., Balsamo, G., Boussetta, S., Choulga, M., Harrigan, S., Hersbach, H., Martens, B., Miralles, D. G., Piles, M., Rodríguez-Fernández, N. J., Zsoter, E., Buontempo, C., and Thépaut, J.-N.: ERA5-Land: a state-of-the-art global reanalysis dataset for land applications, Earth System Science Data, 13, 4349–4383, https://doi.org/10.5194/essd-13-4349-2021, publisher: Copernicus GmbH, 2021.

Noël, B., van de Berg, W. J., van Wessem, J. M., van Meijgaard, E., van As, D., Lenaerts, J. T. M., Lhermitte, S., Kuipers Munneke, P., Smeets, C. J. P. P., van Ulft, L. H., van de Wal, R. S. W., and van den Broeke, M. R.: Modelling the climate and surface mass balance of polar ice sheets using RACMO2 – Part 1: Greenland (1958–2016), The Cryosphere, 12, 811–831, https://doi.org/10.5194/tc-12-811-2018, publisher: Copernicus GmbH, 2018.

Noël, B., van de Berg, W. J., Lhermitte, S., and van den Broeke, M. R.: Rapid ablation zone expansion amplifies north Greenland mass loss, Science Advances, 5, eaaw0123, https://doi.org/10.1126/sciadv.aaw0123, publisher: American Association for the Advancement of Science, 2019.

Obreht, I., De Vleeschouwer, D., Wörmer, L., Kucera, M., Varma, D., Prange, M., Laepple, T., Wendt, J., Nandini-Weiss, S. D., Schulz, H., and Hinrichs, K.-U.: Last Interglacial decadal sea surface temperature variability in the eastern Mediterranean, Nature Geoscience, 15, 812–818, https://doi.org/10.1038/s41561-022-01016-y, number: 10 Publisher: Nature Publishing Group, 2022.

Oerlemans, J. and Knap, W. H.: A 1 year record of global radiation and albedo in the ablation zone of Morteratschgletscher, Switzerland, Journal of Glaciology, 44, 231–238, https://doi.org/10.3189/S0022143000002574, 1998.

Opsteegh, J. D., Haarsma, R. J., Selten, F. M., and Kattenberg, A.: ECBILT: a dynamic alternative to mixed boundary conditions in ocean models, Tellus A: Dynamic Meteorology and Oceanography, 50, 348–367, https://doi.org/10.3402/tellusa.v50i3.14524, number: 3 Publisher: Stockholm University Press, 1998.

https://doi.org/10.5194/egusphere-2024-556
Preprint. Discussion started: 18 March 2024

Otto-Bliesner, B. L., Rosenbloom, N., Stone, E. J., McKay, N. P., Lunt, D. J., Brady, E. C., and Overpeck, J. T.: How warm was the last interglacial? New model–data comparisons, Philosophical Transactions of the Royal Society A: Mathematical, Physical and Engineering Sciences, 371, 20130 097, https://doi.org/10.1098/rsta.2013.0097, publisher: Royal Society, 2013.

Plach, A., Nisancioglu, K. H., Le clec'h, S., Born, A., Langebroek, P. M., Guo, C., Imhof, M., and Stocker, T. F.: Eemian Greenland SMB strongly sensitive to model choice, Climate of the Past, 14, 1463–1485, https://doi.org/10.5194/cp-14-1463-2018, publisher: Copernicus GmbH, 2018.

Quiquet, A., Roche, D. M., Dumas, C., and Paillard, D.: Online dynamical downscaling of temperature and precipitation within the *i*LOVECLIM model (version 1.1), Geoscientific Model Development, 11, 453–466, https://doi.org/10.5194/gmd-11-453-2018, publisher: Copernicus GmbH, 2018.

Quiquet, A., Roche, D. M., Dumas, C., Bouttes, N., and Lhardy, F.: Climate and ice sheet evolutions from the last glacial maximum to the pre-industrial period with an ice-sheet–climate coupled model, Climate of the Past, 17, 2179–2199, https://doi.org/10.5194/cp-17-2179-2021, publisher: Copernicus GmbH, 2021.

Reeh, N.: Parameterization of Melt Rate and Surface Temperature in the Greenland Ice Sheet, https://epic.awi.de/id/eprint/28262/, iSSN: 0032-2490 Issue: 3 Number: 3 Pages: 113-128 Place: Bremerhaven Publisher: Alfred Wegener Institute for Polar and Marine Research & German Society of Polar Research Volume: 59, 1991.

Robinson, A. and Goelzer, H.: The importance of insolation changes for paleo ice sheet modeling, The Cryosphere, 8, 1419–1428, https://doi.org/10.5194/tc-8-1419-2014, publisher: Copernicus GmbH, 2014.

Roche, D. M., Dumas, C., Bügelmayer, M., Charbit, S., and Ritz, C.: Adding a dynamical cryosphere to *i*LOVECLIM (version 1.0): coupling with the GRISLI ice-sheet model, Geoscientific Model Development, 7, 1377–1394, https://doi.org/10.5194/gmd-7-1377-2014, publisher: Copernicus GmbH, 2014a.

Roche, D. M., Paillard, D., Caley, T., and Waelbroeck, C.: LGM hosing approach to Heinrich Event 1: results and perspectives from data–model integration using water isotopes, Quaternary Science Reviews, 106, 247–261, https://doi.org/10.1016/j.quascirev.2014.07.020, 2014b.

Spratt, R. M. and Lisiecki, L. E.: A Late Pleistocene sea level stack, Climate of the Past, 12, 1079–1092, https://doi.org/10.5194/cp-12-1079-2016, 2016.

Stone, E. J., Lunt, D. J., Annan, J. D., and Hargreaves, J. C.: Quantification of the Greenland ice sheet contribution to Last Interglacial sea level rise, Climate of the Past, 9, 621–639, https://doi.org/10.5194/cp-9-621-2013, publisher: Copernicus GmbH, 2013.

Sutter, J., Gierz, P., Grosfeld, K., Thoma, M., and Lohmann, G.: Ocean temperature thresholds for Last Interglacial West Antarctic Ice Sheet collapse, Geophysical Research Letters, 43, 2675–2682, https://doi.org/10.1002/2016GL067818, _eprint: https://onlinelibrary.wiley.com/doi/pdf/10.1002/2016GL067818, 2016.

Tedesco, M., Doherty, S., Fettweis, X., Alexander, P., Jeyaratnam, J., and Stroeve, J.: The darkening of the Greenland ice sheet: trends, drivers, and projections (1981–2100), The Cryosphere, 10, 477–496, https://doi.org/10.5194/tc-10-477-2016, publisher: Copernicus GmbH, 2016.

Turney, C. S. and Jones, R. T.: Does the Agulhas Current amplify global temperatures during super-interglacials?, Journal of Quaternary Science, 25, 839–843, https://doi.org/10.1002/jqs.1423, _eprint: https://onlinelibrary.wiley.com/doi/pdf/10.1002/jqs.1423, 2010.

Turney, C. S. M., Fogwill, C. J., Golledge, N. R., McKay, N. P., van Sebille, E., Jones, R. T., Etheridge, D., Rubino, M., Thornton, D. P., Davies, S. M., Ramsey, C. B., Thomas, Z. A., Bird, M. I., Munksgaard, N. C., Kohno, M., Woodward, J., Winter, K., Weyrich, L. S., Rootes, C. M., Millman, H., Albert, P. G., Rivera, A., van Ommen, T., Curran, M., Moy, A., Rahmstorf, S., Kawamura, K., Hillenbrand,

https://doi.org/10.5194/egusphere-2024-556
Preprint. Discussion started: 18 March 2024

C.-D., Weber, M. E., Manning, C. J., Young, J., and Cooper, A.: Early Last Interglacial ocean warming drove substantial ice mass loss from Antarctica, Proceedings of the National Academy of Sciences, 117, 3996–4006, https://doi.org/10.1073/pnas.1902469117, publisher: Proceedings of the National Academy of Sciences, 2020.

Ullman, D. J., LeGrande, A. N., Carlson, A. E., Anslow, F. S., and Licciardi, J. M.: Assessing the impact of Laurentide Ice Sheet topography on glacial climate, Climate of the Past, 10, 487–507, https://doi.org/10.5194/cp-10-487-2014, publisher: Copernicus GmbH, 2014.

van Dalum, C. T., van de Berg, W. J., and van den Broeke, M. R.: Sensitivity of Antarctic surface climate to a new spectral snow albedo and radiative transfer scheme in RACMO2.3p3, The Cryosphere, 16, 1071–1089, https://doi.org/10.5194/tc-16-1071-2022, publisher: Copernicus GmbH, 2022.

Van Den Berg, J., Van De Wal, R., and Oerlemans, H.: A mass balance model for the Eurasian Ice Sheet for the last 120,000 years, Global and Planetary Change, 61, 194–208, https://doi.org/10.1016/j.gloplacha.2007.08.015, 2008.

Zolles, T. and Born, A.: Sensitivity of the Greenland surface mass and energy balance to uncertainties in key model parameters, The Cryosphere, 15, 2917–2938, https://doi.org/10.5194/tc-15-2917-2021, publisher: Copernicus GmbH, 2021.

Zolles, T. and Born, A.: How does a change in climate variability impact the Greenland ice-sheet surface mass balance?, The Cryosphere Discussions, pp. 1–18, https://doi.org/10.5194/tc-2021-379, publisher: Copernicus GmbH, 2022.